The diameter of hyperbolic random graphs

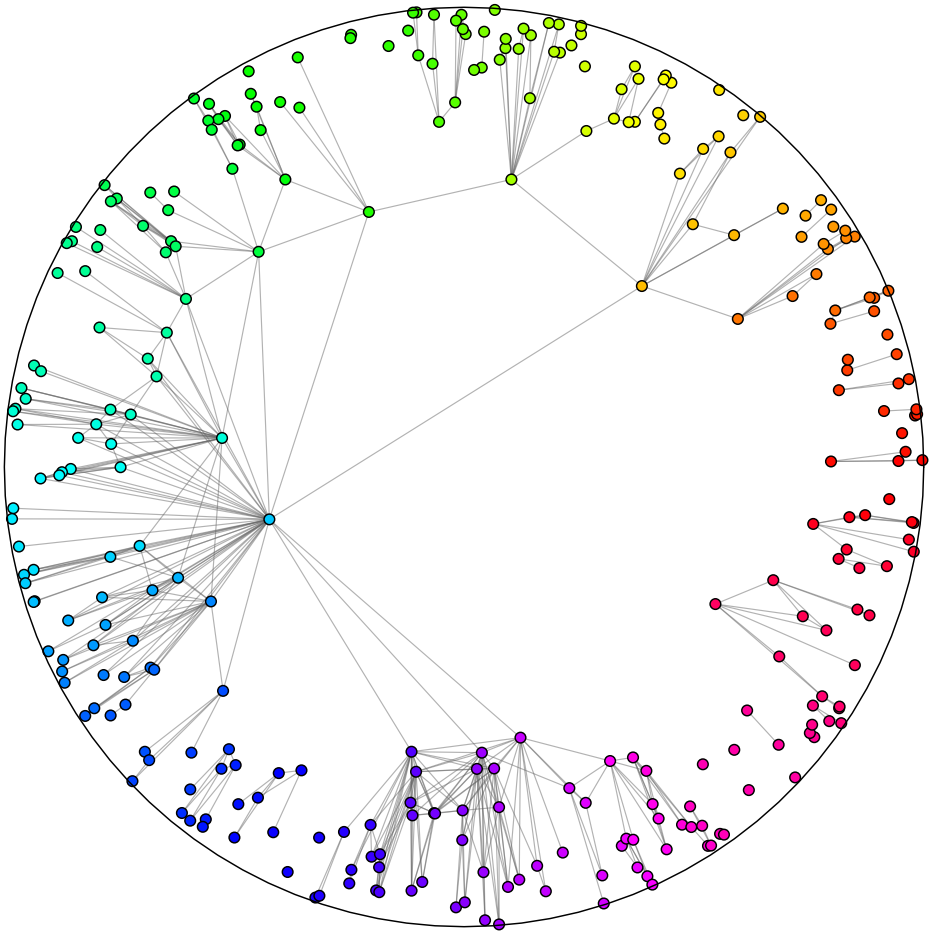

Merlijn Staps
March 27, 2017

Master's thesis
Supervisor: dr. Tobias Müller
Second reader: prof. dr. Roberto Fernández

Utrecht University
Faculty of Science
Department of Mathematics

Merlijn Staps, BSc: *The diameter of hyperbolic random graphs*
Master's thesis, Mathematical Sciences

Supervisor: dr. Tobias Müller
Second reader: prof. dr. Roberto Fernández

Time frame: April 2016 - March 2017

The figure on the front page visualizes a KPKVB random graph in the native representation of the hyperbolic plane. Parameters used are $N = 300$, $\alpha = 0.8$ and $\nu = 1$. Vertices are colored based on their angular coordinate.

Abstract

This thesis was written by Merlijn Staps from April 2016 until March 2017 as part of the master's programme Mathematical Sciences at Utrecht University. The research was supervised by dr. Tobias Müller. The second reader is prof. dr. Roberto Fernández.

We study the graph diameter in the KPKVB model, a recent model of random geometric graphs in the hyperbolic plane that was introduced because it has properties reminiscent of complex networks: it has a power law degree distribution, local clustering and small graph theoretic distances. After introducing the model, we show how it can be approximated by a random geometric graph in the Euclidean plane that turns out to be easier to handle. We then use this approximation to improve previous results on the diameter of KPKVB random graphs, by showing that with probability tending to 1 as $N \to \infty$, the maximum diameter of the components of the graph is at most a constant times $\log N$. Here N denotes the number of vertices. We also provide a logarithmic lower bound for the diameter that holds with probability tending to 1. This lower bound was already known in the literature. Together, this shows that, asymptotically, the graph diameter in the KPKVB model is logarithmic in the number of vertices.

Acknowledgments

This thesis would not have been possible without the help of a number of people. I extend my gratitude to all of them.

First of all, I would like to thank Tobias Müller for being my supervisor and for giving me the opportunity to work on this topic. I greatly benefited from his guidance and his helpful suggestions during our meetings. I am also grateful for the opportunity to present my work at the STAR Workshop on Random Graphs, held in Utrecht on January 26 and 27, 2017.

I would like to thank Roberto Fernández for being the second reader of this thesis.

I also had a lot of fun discussions with fellow students, often in the wonderful library of the Mathematical Institute. I would like to thank all of them for their input. In particular, I thank Jan-Willem van Ittersum, Harry Smit and Marieke van der Wegen, who took the time to read parts of the manuscript and provided many valuable comments.

Contents

Introduction

A graph is the mathematical formalization of a network. It consists of vertices (points) and edges (lines) connecting those vertices. For example, a social network can be modeled as a graph in which the vertices represent people and the edges connect people that are friends of each other. A random graph is a graph that is constructed through some random process. Both the vertices and the edges of a random graph can be random.

A simple random graph model is the Erdős-Renyi model. In this model, a graph is constructed by starting with a fixed number of vertices and connecting each pair of vertices independently with some fixed probability p. The structure of the resulting graph is usually studied asymptotically, with the number of vertices tending to infinity.

The vertices of a random geometric graph are chosen randomly in some metric space. Edges are then drawn between vertices that are close to each other in the ambient space. For example, one could sample independent points from the unit square and then connect pairs of points with distance at most some threshold d. Random geometric graphs behave differently from Erdős-Renyi random graphs. Unlike Erdős-Renyi random graphs, they exhibit clustering: vertices with a common neighbor have a higher probability of being neighbors as well (because they tend to be close to each other in the ambient space). Furthermore, "not all vertices are the same": the properties of vertices may depend on where they land in space.

In this thesis we consider a random geometric graph that is not constructed in Euclidean space, but in the hyperbolic plane. In particular, we consider a model for random hyperbolic graphs introduced by Krioukov et al. [21] that turns out to have characteristics similar to those of so-called complex networks. In this thesis we study the diameter in this random graph model. The diameter of a graph is the minimal value of d such that between any two vertices between which a path exists in the graph, there exists such a path consisting of at most d edges. In other words, the diameter is the length of the longest shortest path in the graph.

In Chapter 1 we discuss some tools and concepts that we will need in the remainder of the thesis. Section 1.1 provides a brief introduction to the concept of complex networks. In Section 1.2 we set up hyperbolic geometry and derive some of its properties. We also introduce the Poincaré disk representation of the hyperbolic plane, which we will use when defining our random graph model. In Section 1.3 we give a formal introduction into Poisson point processes. This framework will be used later to handle random sets of points.

In Chapter 2 we introduce the KPKVB model [21], which is the random graph model that we are concerned with in this thesis. After setting it up in Section 2.1 we give an overview of the known results on this model. Section 2.2 contains some necessary calculations that will be used to study the model. In Section 2.3 we introduce a second random geometric graph that was introduced in [11] and can be used as an approximation for the KPKVB model.

In Chapter 3 we study the diameter of the KPKVB model. We start by presenting an asymptotic logarithmic lower bound for the diameter, which was proven in [19] and [12]. This logarithmic lower bound is the topic of Section 3.1. In Section 3.2, we prove the original result of this thesis, which is a matching asymptotic logarithmic upper bound for the diameter that holds with probability 1 as the number of vertices tends to infinity.

Prerequisites

We assume that the reader is familiar with abstract measure theory and (measure theoretic foundations of) probability theory. We also assume some familiarity with basic concepts from graph theory. We do not assume previous experience with hyperbolic geometry and provide an introduction to the hyperbolic plane in Section 1.2.

Notation

Since we study the asymptotic behavior of random graphs, we frequently make use of asymptotic notation. We always take the limit $N \to \infty$ (or, equivalently, $R \to \infty$, see Section 2.1), where N is the number of vertices. When f, g are real-valued functions of R with g nonnegative, we write

- $f(R) = O(g(R))$ if there exists a constant $C > 0$ such that for all sufficiently large R it holds that $0 \leq f(R) \leq Cg(R)$;
- $f(R) = \Omega(g(R))$ if there exists a constant $C > 0$ such that for all sufficiently large R it holds that $Cg(R) \leq f(R)$;
- $f(R) = o(g(R))$ if we have $\lim_{R\to\infty} f(R)/g(R) = 0$;
- $f(R) = \Theta(g(R))$ if both $f(R) = O(g(R))$ and $f(R) = \Omega(g(R))$, that is, if there are positive constants C_1 and C_2 such that $C_1 g(R) \leq f(R) \leq C_2 g(R)$ for all sufficiently large R.

Formally, $O(g(R))$, $\Omega(g(R))$, $\Theta(g(R))$ and $o(g(R))$ should be seen as *classes* of functions (and it would maybe be better to use an $\in$ symbol instead of an $=$ symbol). By $O(g(R))$ we can also mean "some member of $O(g(R))$", so when we write $f(R) = 1 + O(R)$ we mean that $f(R) - 1$ is a function that belongs to $O(R)$.

Sometimes we also use this notation in a non-asymptotic sense; in this case an expression like $f(a) = O(g(a))$ just means that for some $C > 0$ we have $0 \leq f(a) \leq Cg(a)$ for all a. This use should be clear from context. When X is some random variable defined on our random graph, we will also encounter statements of the form $\mathbb{P}(X = O(R)) \to 1$, which is to be read as: there exists a positive constant C such that $\mathbb{P}(0 \leq X \leq CR)$ has limit 1 for $R \to \infty$.

By $|a - b|_d$ we will mean the distance between two real numbers a and b, taken modulo d:

$$|a - b|_d = \min_{k\in\mathbb{Z}} |a - b + kd|.$$

If we are given a sequence of probability spaces $(\Omega_n, \mathcal{F}_n, \mathbb{P}_n)_{n\geq 1}$ and an event X that can be defined on each of them, then we say that X happens *asymptotically almost surely* or *a.a.s.* if $\mathbb{P}_n(X) \to 1$ as $n \to \infty$.

1

Preliminaries

This chapter consists of three independent sections. In Section 1.1 we give an introduction into complex networks. In Section 1.2 we introduce the hyperbolic plane. In Section 1.3 we formally introduce the Poisson point process.

1.1 Complex networks

The term *complex network* refers to real-world networks that share a number of graph-theoretic characteristics despite arising in completely different contexts. The list of examples includes social networks, the internet, metabolic networks, protein interaction networks, neural networks, collaboration networks of scientists and many more [2, 25, 28].

The common characteristics of complex networks include the following:

1. the network has a *large* number of nodes;
2. the network is *sparse*, which means that the number of connections is a small multiple of the number of nodes. In other words, the average number of neighbors of a node is small;
3. the network exhibits *local clustering*, which means that nodes with a common neighbor have a higher probability of being connected;
4. there are *small distances*, which means that there are short paths in the network between most pairs of nodes;
5. the degree distribution follows a *power law*, which means that the number of nodes of degree k is proportional to $k^{-\beta}$ for some exponent $\beta \geq 1$. As a consequence, most nodes have very small degree, but there are a few nodes (called "hubs") with very large degree.

Properties 3 and 4 are together referred to as the "small-world phenomenon" [28]. The power law degree distribution is sometimes also referred to as a "scale-free degree distribution" [2]. The terms "small-world network" and "scale-free network" are also used to describe complex networks.

As an example, we consider the network with as nodes all people in The Netherlands, where two people are connected by an edge if they know each other. This is an example of a social network. Having millions of nodes, the network clearly satisfies 1. It can also be called sparse (property 2), because most people in The Netherlands know only a very small fraction of fellow Dutchmen. The clustering property (property 3) arises from the fact that common acquaintances of a person have a higher probability of also knowing each other, because they may for instance all three live in the same city or work at the same place. Small distances (property 4) in social networks were famously demonstrated in experiments by Stanley Milgram in the United States [23]. The results of these experiments have become known under the slogan "six degrees of separation", which means that most pairs of people are connected to each other via a sequence of at most six "friends of friends". Large social networks often do not have property 5 however, because the degree distribution in a social network is typically Gaussian [25].

As a second example, we consider a network from logistics. The nodes of this network are all airports in the world, and two airports are connected if there are regular flights between the two. This network clearly has properties 1 and 2. Property 3 arises from the fact that airports from

which flights exist to the same airport are generally close geographically. Property 4 translates to the phenomenon that for most pairs of airports a short (in terms of number of flights) sequence of flights can be taken from the one to the other. The airport network also has a power law degree distribution [15]. Most airports will be local airports with a small number of connections, but there are nodes with a very large degree: these are large international airports such as Schiphol Airport.

Mathematical descriptions of complex networks characteristics

We now discuss how the properties described above can be translated into the language of graph theory. The sparseness of a network can be measured by the average degree. If a random graph model for complex networks has a variable number of vertices N, then the sparseness condition could be that the average degree stays bounded for $N \to \infty$.

The clustering property is usually measured by the average *clustering coefficient*. Between the neighbors of a node with degree k, there are $\binom{k}{2}$ potential connections. The fraction of those connections that are present in the network is called the clustering coefficient of the node. The clustering coefficient of the network then is the average clustering coefficient over all nodes.

The distance between two nodes in the network can be measured by the number of edges in the shortest path between the nodes (this distance may be infinite if no such path exists). To obtain a parameter that describes the whole network, one can either take the average over all finite distances between pairs of nodes (the "typical distance") or the maximum distance (the diameter). For a small-world network, the typical distance is on the order of $\log N$ or even $\log \log N$ [26].

The power law condition was already formalized mathematically above; it is a condition on the degree sequence of the graph.

Models of complex networks

An obvious question is why complex networks, despite coming from completely different areas of science, share many characteristics. Network scientists have searched for a model of complex networks that explains how these characteristics may arise.

The most natural random graph model, the Erdős-Renyi model, is certainly not a good model for complex networks. Recall that in this model a graph is constructed on N vertices by drawing each possible edge independently with probability p. Although N and p can be chosen such that property 1 and 2 are satisfied, Erdős-Renyi graphs do not exhibit clustering or a power-law degree distribution.

The Chung–Lu model for random graphs is a model that does give a power-law degree distribution [7]. Contrary to the Erdős-Renyi model, this is an inhomogeneous random graph model in the sense that the expected degree is not the same for each vertex. In the Chung–Lu model, each of the N vertices $v_1, \ldots, v_N$ comes with a weight w_i. The connection probability of vertices v_i and v_j is now proportional to $w_i w_j$. The weights can be chosen in such a way that the resulting random graph has a power law degree distribution.

Barabási and Albert [2] suggested that complex networks may arise through a process called *preferential attachment*. This process describes the evolution of a graph through the following two mechanisms: (i) vertices are added one by one and (ii) once a new vertex is added, it is connected to some of the already existing vertices with a preference for vertices that already have many connections. Like the Chung–Lu model, the preferential attachment model can also give rise to a power-law degree distribution.

Krioukov et al. [21] suggested that complex networks may have a hidden underlying hyperbolic geometry and introduced a random geometric graph model in the hyperbolic plane that exhibits

the characteristics described above. The random graph model they introduced is the subject of this thesis. We introduce their model in Chapter 2.

1.2 Hyperbolic geometry

In this section we set up the hyperbolic plane and discuss a few basic properties of it. Most of the results and statements of this chapter are from lecture notes by Walkden [27]. A more historical introduction to the topic of hyperbolic geometry can be found in the book by Stillwell [24].

The hyperbolic plane is a surface of constant negative curvature -1. In contrast, the Euclidean plane is a surface of zero curvature and the sphere is a surface of constant curvature 1. A classical result by Hilbert [16] is that there is no complete analytic regular surface in 3-dimensional Euclidean space $\mathbb{R}^3$ of constant negative curvature. Consequently, there is no isometric embedding of class $\mathcal{C}^\infty$ of the hyperbolic plane into $\mathbb{R}^3$. There are however many equivalent models of the hyperbolic plane as subsets of Euclidean spaces, each of which emphasizes some of its properties. The model we will most frequently make use of is the Poincaré disk model, which is a representation of the hyperbolic plane inside the unit disk in the Euclidean plane. The model we will start from, however, is the Poincaré half plane model, which represents the hyperbolic plane as the upper (Euclidean) half plane.

In Section 2.1 we will construct a random graph on a disk in the hyperbolic plane. The critical property of hyperbolic geometry that we will use is that the perimeter of such a disk grows exponentially with the radius (see Lemma 1.2.11 below). This means that if points are distributed uniformly over the disk, most points will end up close to the boundary. If points at close hyperbolic distance are connected by an edge, points close to the center will typically have a high degree, whereas points close to the boundary will have a low degree (close to the boundary distances are "larger" because perimeter increases exponentially). As a consequence, one ends up with a graph where most vertices have small degree, whereas a few vertices have large degree. Furthermore, the graph naturally exhibits local clustering. This is in a nutshell the idea behind modeling complex networks with hyperbolic random graphs [21].

Hyperbolic distances in the upper half-plane

A model for the hyperbolic plane is obtained when the upper half plane $\mathbb{H} = \{z \in \mathbb{C} : \operatorname{Im} z > 0\}$ is equipped with the metric defined by the differential form $\mathrm{d}s = \mathrm{d}z/\operatorname{Im} z$. This means that the hyperbolic length $\ell_{\mathbb{H}}(\gamma)$ of a (continuous) path $\gamma : [0,1] \to \mathbb{H}$ is obtained by integrating the function $1/(\operatorname{Im} z)$ along γ:

$$\ell_{\mathbb{H}}(\gamma) = \int_\gamma \frac{1}{\operatorname{Im} z}\,\mathrm{d}\gamma = \int_0^1 \frac{|\gamma'(t)|}{\operatorname{Im}\gamma(t)}\,\mathrm{d}t.$$

The hyperbolic distance $d_{\mathbb{H}}(z_1, z_2)$ between two points z_1, $z_2 \in \mathbb{H}$ is now naturally defined as the infimum over the hyperbolic lengths of all possible continuous paths from z_1 to z_2.

Our first task is to find the path of shortest length between two arbitrary points z_1, $z_2 \in \mathbb{H}$. Such a path is called a *geodesic*. We first show that for two points $z_1 = ia$, $z_2 = ib$ (where $b > a$), the geodesic is given by the vertical line segment from z_1 to z_2.

Lemma 1.2.1 ([27], Proposition 4.2.1)**.** *Let $a < b$. The geodesic between $z_1 = ia$ and $z_2 = ib$ is given by the imaginary axis. The hyperbolic distance between z_1 and z_2 is* $\log(b/a)$.

Proof. First consider the path $\gamma : [a, b] \to \mathbb{H}$ from z_1 to z_2 given by $\gamma : t \mapsto it$. The hyperbolic length of this path is given by $\ell_{\mathbb{H}}(\gamma) = \int_a^b \frac{1}{\operatorname{Im}\gamma(t)}\,\mathrm{d}t = \int_a^b \frac{1}{t}\,\mathrm{d}t = \log(b/a)$. It remains to show that

no other path from z_1 to z_2 has smaller length. Consider any path $\gamma : [0,1] \to \mathbb{H}$ with $\gamma(0) = z_1$ and $\gamma(1) = z_2$. Write $\gamma(t) = x(t) + iy(t)$. The length of the path is now given by

$$\begin{aligned}\ell_{\mathbb{H}}(\gamma) &= \int_0^1 \frac{\sqrt{x'(t)^2 + y'(t)^2}}{y(t)}\,\mathrm{d}t \geq \int_0^1 \frac{\sqrt{y'(t)^2}}{y(t)}\,\mathrm{d}t \\ &= \int_0^1 \frac{|y'(t)|}{y(t)}\,\mathrm{d}t \geq \int_0^1 \frac{y'(t)}{y(t)}\,\mathrm{d}t = \log(b) - \log(a) = \log(b/a),\end{aligned}$$

as required. Equality holds provided that $y'(t)$ is nonnegative and $x'(t) = 0$, which means that the path should follow the vertical axis. □

We have now found the geodesic between points on the imaginary axis. We claim that the geodesic between two arbitrary points is either a vertical line or a circle orthogonal to the horizontal axis.

By a Möbius transformation of $\mathbb{H}$ we mean a fractional transformation of the form $f(z) = \frac{az+b}{cz+d}$, where a, b, c, d are real numbers such that $ad - bc$ is nonzero. We call $ad - bc$ the *determinant* of the transformation. If the determinant is positive, f is a bijective transformation of $\mathbb{H}$ onto itself. It is easy to check that the Möbius transformations with positive determinant form a group under composition of functions.

Lemma 1.2.2 ([27], Proposition 4.1.1)**.** *Möbius transformations preserve hyperbolic distances: if f is a Möbius transformation with positive determinant, then $d_{\mathbb{H}}(z_1, z_2) = d_{\mathbb{H}}(f(z_1), f(z_2))$.*

Proof. It suffices to prove that f preserves the length of any path in $\mathbb{H}$ from z_1 to z_2. Consider such a path $\gamma : [0,1] \to \mathbb{H}$ where $\gamma(0) = z_1$ and $\gamma(1) = z_2$. Then

$$\ell_{\mathbb{H}}(\gamma) = \int_0^1 \frac{|\gamma'(t)|}{\operatorname{Im}\gamma(t)}\,\mathrm{d}t.$$

We now compute the length of the path $f(\gamma)$ (because f has positive determinant, this also is a path in $\mathbb{H}$). Notice that

$$\ell_{\mathbb{H}}(f(\gamma)) = \int_0^1 \frac{|(f\circ\gamma)'(t)|}{\operatorname{Im} f(\gamma(t))}\,\mathrm{d}t = \int_0^1 \frac{|f'(\gamma(t))||\gamma'(t)|}{\operatorname{Im} f(\gamma(t))}\,\mathrm{d}t.$$

Write $f(z) = \frac{az+b}{cz+d}$. Then we have

$$f'(z) = \frac{a(cz+d) - c(az+b)}{(cz+d)^2} = \frac{ad-bc}{(cz+d)^2}$$

and

$$\operatorname{Im} f(z) = \operatorname{Im}\left(\frac{az+b}{cz+d}\right) = \frac{1}{|cz+d|^2}\operatorname{Im}\left((az+b)(c\overline{z}+d)\right) = \frac{ad-bc}{|cz+d|^2}\operatorname{Im} z.$$

Therefore, from $\ell_{\mathbb{H}}(f(\gamma)) = \int_0^1 \frac{|f'(\gamma(t))||\gamma'(t)|}{\operatorname{Im} f(\gamma(t))}\,\mathrm{d}t$ and the fact that $ad - bc > 0$, it follows that

$$\ell_{\mathbb{H}}(f(\gamma)) = \int_0^1 \frac{ad-bc}{|d+c\gamma(t)|^2}\cdot|\gamma'(t)|\cdot\frac{|d+c\gamma(t)|^2}{(ad-bc)\cdot\operatorname{Im}\gamma(t)}\,\mathrm{d}t = \int_0^1 \frac{|\gamma'(t)|}{\operatorname{Im}\gamma(t)}\,\mathrm{d}t = \ell_{\mathbb{H}}(\gamma),$$

as desired. □

Lemma 1.2.3 ([27], Lemma 5.2.1)**.** *Let z_1, $z_2 \in \mathbb{H}$ be distinct. Then there exists a Möbius transformation f with positive determinant that maps z_1 to i and z_2 to a point on the imaginary axis that lies above i.*

Proof. Note that horizontal translations and dilations centred at the origin are Möbius transformations. It follows that there exists a Möbius transformation that maps z_1 to i. Therefore, we may assume that $z_1 = i$ and show that there exists a Möbius transformation that leaves i fixed and maps z_2 to a point on the imaginary axis. Write $w = z_2$. Note that the quadratic polynomial

$$Q(T) = T^2 \operatorname{Re} w + T(1 - |w|^2) - \operatorname{Re} w$$

has nonnegative discriminant $(1 - |w|^2)^2 + (2 \operatorname{Re} w)^2$. Therefore, Q has some real zero $T = a$. We claim that the Möbius transformation $f(z) = \frac{az+1}{-z+a}$ has the required property that $f(w)$ lies on the imaginary axis. Note that this Möbius transformation has positive determinant $a^2 + 1$ and that $f(i) = \frac{ai+1}{a-i} = i$. It remains to compute the real part of $f(w)$ to show that $f(w)$ lies on the imaginary axis. We have

$$f(w) = \frac{aw+1}{a-w} = \frac{aw+1}{a-w} \cdot \frac{\overline{a-w}}{\overline{a-w}} = \frac{(aw+1) \cdot \overline{(a-w)}}{|a-w|^2}.$$

We have $(aw+1) \cdot \overline{(a-w)} = a^2 w - a|w|^2 + a - \overline{w}$ with real part $a^2 \operatorname{Re}(w) + a(1 - |w|^2) - \operatorname{Re} w = 0$ by the choice of a. Thus $f(z_2) = f(w)$ lies on the imaginary axis. If $f(w)$ lies above i, we are done. If $f(w)$ lies below i, we next apply the Möbius transformation $z \mapsto \frac{-1}{z}$ with determinant 1. This transformation leaves i fixed and sends $f(w)$ to a point on the imaginary axis that lies above i. □

Theorem 1.2.4 ([27], Theorem 5.2.2)**.** *Let z_1, $z_2 \in \mathbb{H}$. The unique geodesic in $\mathbb{H}$ connecting z_1 and z_2 is either a vertical line or a semicircle orthogonal to the horizontal axis.*

Proof. By Lemma 1.2.3, there exists a Möbius transformation f such that $f(z_1) = i$ and $f(z_2) = ti$ for some positive t. By Lemma 1.2.1, the vertical axis is the unique geodesic through z_1 and z_2. Applying f^{-1}, we see by using Lemma 1.2.2 that the unique geodesic between z_1 and z_2 is the image of the vertical axis under the Möbius transformation f^{-1}. Write $f^{-1}(z) = \frac{az+b}{cz+d}$. If $c = 0$ or $d = 0$ then the image of the imaginary axis under f^{-1} is another vertical line. If $cd \neq 0$ we claim that the image of the imaginary axis under f^{-1} is a semicircle centred at $\frac{ad+bc}{2cd}$. Indeed, if z lies on the imaginary axis then

$$\begin{aligned} \frac{az+b}{cz+d} - \frac{ad+bc}{2cd} &= \frac{2cd(az+b) - (cz+d)(ad+bc)}{2cd(cz+d)} \\ &= \frac{(ad-bc)(cz-d)}{2cd(cz+d)} = \frac{ad-bc}{2cd} \cdot \frac{cz-d}{cz+d} \end{aligned}$$

which has absolute value $\frac{ad-bc}{2cd}$ since z lies on the imaginary axis. So the distance from $f^{-1}(z)$ to the point $\frac{ad+bc}{2cd}$ on the real axis is independent of z, which means that f^{-1} maps the imaginary axis to a semicircle centred at $\frac{ad+bc}{2cd}$. This semicircle is orthogonal to the real axis. □

We will also refer to the geodesics as *hyperbolic lines*. Having found the geodesics, we can compute the hyperbolic distance between any two points.

Theorem 1.2.5. *The hyperbolic distance between z_1, $z_2 \in \mathbb{H}$ satisfies*

$$\cosh d_{\mathbb{H}}(z_1, z_2) = 1 + \frac{|z_1 - z_2|^2}{2(\operatorname{Im} z_1)(\operatorname{Im} z_2)}.$$

Proof. If $\operatorname{Re} z_1 = \operatorname{Re} z_2$ the geodesic between z_1 and z_2 is a vertical line and by a similar argument as in the proof of Lemma 1.2.1 we find that $d_{\mathbb{H}}(z_1, z_2) = \log(\operatorname{Im} z_1 / \operatorname{Im} z_2)$ (where we assume $\operatorname{Im} z_1 \geq \operatorname{Im} z_2$). We find

$$\cosh d_{\mathbb{H}}(z_1, z_2) = \frac{(\operatorname{Im} z_1)^2 + (\operatorname{Im} z_2)^2}{2(\operatorname{Im} z_1)(\operatorname{Im} z_2)} = 1 + \frac{|z_1 - z_2|^2}{2(\operatorname{Im} z_1)(\operatorname{Im} z_2)}.$$

If $\operatorname{Re} z_1 \neq \operatorname{Re} z_2$ the geodesic connecting z_1 and z_2 is a semicircle orthogonal to the real axis centered at a certain point $p \in \mathbb{R}$. Write $z_k = p + re^{\varphi_k i}$ for $k = 1, 2$ and define the path $\gamma : [\varphi_1, \varphi_2] \to \mathbb{H}$ given by $t \mapsto p + re^{ti}$ (we may assume $0 < \varphi_1 \leq \varphi_2 < \pi$). This path satisfies $\gamma(\varphi_1) = z_1$, $\gamma(\varphi_2) = z_2$ and follows the geodesic between z_1 and z_2, so we obtain

$$\begin{aligned} d_{\mathbb{H}}(z_1, z_2) = \ell_{\mathbb{H}}(\gamma) &= \int_{\varphi_1}^{\varphi_2} \frac{|\gamma'(t)|}{\operatorname{Im}\gamma(t)}\,\mathrm{d}t \\ &= \int_{\varphi_1}^{\varphi_2} \frac{\sqrt{r^2\sin^2 t + r^2\cos^2 t}}{r\sin t}\,\mathrm{d}t \\ &= \int_{\varphi_1}^{\varphi_2} \frac{1}{\sin t}\,\mathrm{d}t \\ &= \log\left(\frac{\sin\varphi_2}{1+\cos\varphi_2}\right) - \log\left(\frac{\sin\varphi_1}{1+\cos\varphi_1}\right) = \log\left(\frac{\sin\varphi_2(1+\cos\varphi_1)}{\sin\varphi_1(1+\cos\varphi_2)}\right) \end{aligned}$$

because $x \mapsto \log(\frac{\sin x}{1+\cos x})$ is an antiderivative of $x \mapsto \frac{1}{\sin x}$. Indeed,

$$\frac{d}{dx}\log\left(\frac{\sin x}{1+\cos x}\right) = \frac{1+\cos x}{\sin x} \cdot \frac{(1+\cos x)\cos x + \sin^2 x}{(1+\cos x)^2} = \frac{1}{\sin x}.$$

It follows that

$$\begin{aligned} \cosh d_{\mathbb{H}}(z_1, z_2) &= \cosh\left(\log\left(\frac{\sin\varphi_2(1+\cos\varphi_1)}{\sin\varphi_1(1+\cos\varphi_2)}\right)\right) \\ &= \frac{\sin\varphi_2(1+\cos\varphi_1)}{2\sin\varphi_1(1+\cos\varphi_2)} + \frac{\sin\varphi_1(1+\cos\varphi_2)}{2\sin\varphi_2(1+\cos\varphi_1)} \\ &= \frac{(1-\cos\varphi_2)(1+\cos\varphi_1)}{2\sin\varphi_1\sin\varphi_2} + \frac{(1-\cos\varphi_1)(1+\cos\varphi_2)}{2\sin\varphi_2\sin\varphi_1} \\ &= 1 + \frac{(\cos\varphi_1 - \cos\varphi_2)^2 + (\sin\varphi_1 - \sin\varphi_2)^2}{2\sin\varphi_1\sin\varphi_2} \\ &= 1 + \frac{|z_1 - z_2|^2}{2(\operatorname{Im} z_1)(\operatorname{Im} z_2)}, \end{aligned}$$

as desired. In the third step we used that $\frac{\sin x}{1+\cos x} = \frac{1-\cos x}{\sin x}$. □

Hyperbolic triangles

In this paragraph we derive some hyperbolic triangle geometry and trigonometry. We define the (hyperbolic) angle between two paths that meet at $z \in \mathbb{H}$ to be the (Euclidean) angle between their tangent vectors. A very important point is that Möbius transformations are *conformal*, i.e. they preserve angles. This is a consequence of the fact that any complex differentiable function is conformal [22, p. 35].

Consider a right-angled triangle with vertices A, B, $C \in \mathbb{H}$ with a right angle at C. By Lemma 1.2.3, there exist a Möbius transformation that maps C to i and A to a point ki on the imaginary axis. Because there is a right angle at C and the Möbius transformation is conformal, the point $B = s + ti$ now lies on the unit circle (Figure 1.1).

Lemma 1.2.6 (Hyperbolic Pythagoras)**.** *If a hyperbolic triangle ABC has a right angle at C we have* $\cosh c = \cosh a \cosh b$.

Here a, b and c denote the lengths of the sides opposite A, B and C, respectively.

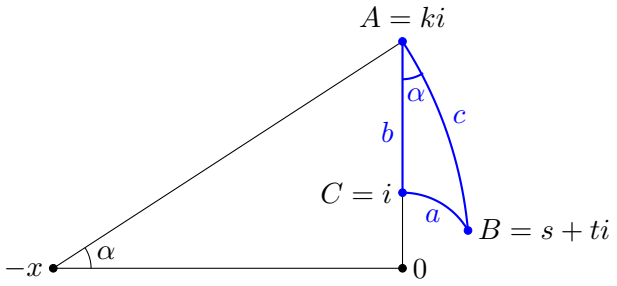

Figure 1.1: A right-angled triangle ABC in the hyperbolic plane. Applying a Möbius transformation, we may assume that $C = i$, $A = ki$ $(k > 1)$ and that $B = s + ti$ lies on the unit circle. The side lengths of triangle ABC are called a, b and c and α is the hyperbolic angle at vertex A. The points 0 and $-x$ are used in the proof of Lemma 1.2.7.

Proof. We may assume that $C = i$, $A = ki$ and $B = s + ti$ with $k > 1$ and $s^2 + t^2 = 1$ (Figure 1.1). Using Theorem 1.2.5 we find $\cosh b = 1 + \frac{(k-1)^2}{2k} = \frac{1+k^2}{2k}$, $\cosh a = 1 + \frac{s^2+(t-1)^2}{2t} = 1 + \frac{2-2t}{2t} = \frac{1}{t}$ and therefore

$$\cosh c = 1 + \frac{s^2 + (t-k)^2}{2tk} = 1 + \frac{1 - 2tk + k^2}{2tk} = \frac{k^2+1}{2tk} = \cosh a \cosh b,$$

as required. □

Lemma 1.2.7 (Hyperbolic trigonometry)**.** *If a hyperbolic triangle ABC has a right angle at C and angle α at A we have*

$$\sin\alpha = \frac{\sinh a}{\sinh c}, \quad \cos\alpha = \frac{\tanh b}{\tanh c} \quad \textit{and} \quad \tan\alpha = \frac{\tanh a}{\sinh b}.$$

Proof. As in the proof of Lemma 1.2.6, we assume that $C = i$, $A = ki$ and $B = s + ti$ with $k > 1$ and $s^2 + t^2 = 1$. We assume the triangle to be non-degenerate, which implies $s \neq 0$. Without loss of generality we assume that s is positive. The geodesic through A and B is a semicircle centered at a point $-x$ at the real axis (again see Figure 1.1). Because $-x$ is equidistant from A and B we have $k^2 + x^2 = t^2 + (s + x)^2$ or $x = \frac{k^2-1}{2s}$. From $k > 1$ and $s > 0$ it follows that x is positive. The points $X = -x$, $A = ki$ and $O = 0$ form a triangle in the Euclidean plane that has a right angle at O. Because the half-plane model of the hyperbolic plane is conformal (hyperbolic angles are Euclidean angles), α is equal to the angle between the line OA and the perpendicular to AX at A. Because OX is perpendicular to AO, it follows that the angle at X in triangle OXA is also equal to α. It follows that $\tan\alpha = \frac{k}{x}$. Note that $\cosh a = \frac{1}{t}$ as in the proof of Lemma 1.2.6. Because a is positive, we have

$$\sinh a = \sqrt{\cosh^2 a - 1} = \sqrt{\frac{1-t^2}{t^2}} = \frac{s}{t},$$

whence $\tanh a = \frac{\sinh a}{\cosh a} = \frac{s/t}{1/t} = s$. Similarly, from $\cosh b = \frac{1+k^2}{2k}$ we have

$$\sinh b = \sqrt{\left(\frac{1+k^2}{2k}\right)^2 - 1} = \frac{k^2-1}{2k}.$$

Because $x = \frac{k^2-1}{2s}$, it follows that

$$\frac{\tanh a}{\sinh b} = \frac{2ks}{k^2-1} = \frac{2ks}{2sx} = \frac{k}{x} = \tan\alpha,$$

which proves the third equality. We now simultaneously prove the first and second equality. Let $A = \frac{\sinh a}{\sinh c}$ and $B = \frac{\tanh b}{\tanh c}$. Note that $A > 0$. We also have $\sin\alpha > 0$ because $\alpha < \frac{\pi}{2}$. We have

$$\frac{A}{B} = \frac{\sinh a \tanh c}{\sinh c \tanh b} = \frac{\sinh a \cosh b}{\cosh c \sinh b} = \frac{\sinh a \cosh b}{\cosh a \cosh b \sinh b} = \frac{\tanh a}{\sinh b} = \tan\alpha,$$

by Lemma 1.2.6 and the equality $\frac{\tanh a}{\sinh b} = \tan\alpha$ which we already deduced above. Note that $\sinh^2 c = \cosh^2 c - 1 = (\frac{k^2+1}{2tk})^2 - 1$, because from the proof of Lemma 1.2.6 we have $\cosh c = \frac{k^2+1}{2tk}$. Furthermore, we have $\sinh^2 a = \frac{s^2}{t^2} = \frac{1-t^2}{t^2}$ and $\tanh^2 b = \frac{\sinh^2 b}{\cosh^2 b} = \frac{(k^2-1)^2}{(k^2+1)^2}$. We obtain

$$\begin{aligned} A^2 + B^2 &= \frac{\sinh^2 a}{\sinh^2 c} + \frac{\tanh^2 b}{\tanh^2 c} = \frac{\sinh^2 a + \cosh^2 c \tanh^2 b}{\sinh^2 c} \\ &= \frac{\frac{1-t^2}{t^2} + \left(\frac{k^2+1}{2tk}\right)^2 \cdot \frac{(k^2-1)^2}{(k^2+1)^2}}{\left(\frac{k^2+1}{2tk}\right)^2 - 1} = \frac{4k^2(1-t^2) + (k^2-1)^2}{(1+k^2)^2 - 4k^2t^2} = 1. \end{aligned}$$

We now have $A^2 + B^2 = 1 = \sin^2\alpha + \cos^2\alpha$ and $A/B = \tan\alpha = \sin\alpha/\cos\alpha$. Because A and $\sin\alpha$ also have the same sign, this leads to the conclusion $(A, B) = (\sin\alpha, \cos\alpha)$, which proves the first and second equality. □

Lemma 1.2.8. *Let ℓ be a hyperbolic line and let $P \in \mathbb{H}$ be a point. Then there exists a hyperbolic line ℓ' containing P that is perpendicular to P.*

Proof. By Lemma 1.2.3, there is a Möbius transformation f with positive determinant that maps ℓ to the vertical axis. Let $P' = f(P)$. The semicircle centered at the origin through P' is perpendicular to the vertical axis. The image of this semicircle under f^{-1} is the desired hyperbolic line ℓ' (we use again that Möbius transformations are conformal). □

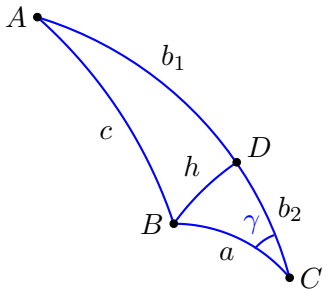

Figure 1.2: Proving the hyperbolic cosine rule. The point D lies on AC such that the hyperbolic lines BD and AC are perpendicular, forming two hyperbolic right triangles ABD and BCD.

Theorem 1.2.9 (Hyperbolic Cosine Rule)**.** *Let ABC be a triangle in $\mathbb{H}$ with angle γ at C. Then we have*

$$\cosh c = \cosh a \cosh b - \sinh a \sinh b \cos\gamma.$$

Proof. By Lemma 1.2.8, the hyperbolic line AC contains a point D such that the hyperbolic line BD is perpendicular to the hyperbolic line AC (Figure 1.2). Let b_1 be the hyperbolic distance between A and D and let b_2 be the hyperbolic distance between C and D. We assume that D lies

in between A and C. Then we have $b = b_1 + b_2$. Let h be the hyperbolic distance between B and D. By Lemma 1.2.6, we have

$$\begin{aligned}\cosh c &= \cosh h \cosh b_1 = \cosh h \cosh(b - b_2) \\ &= \cosh h \left(\cosh b \cosh b_2 - \sinh b \sinh b_2\right).\end{aligned}$$

Since $\cosh a = \cosh h \cosh b_2$, we obtain

$$\begin{aligned}\cosh c &= \cosh b \cosh a - \sinh b \cosh a \tanh b_2 \\ &= \cosh b \cosh a - \sinh a \sinh b \cdot \frac{\tanh b_2}{\tanh a} \\ &= \cosh b \cosh c - \sinh b \sinh c \cos\gamma\end{aligned}$$

where we used Lemma 1.2.7 for the final step.

If A lies between C and D then we have $b_1 = b_2 - b$. Because $\cosh(b_2 - b) = \cosh(b - b_2)$ the proof is exactly the same.

Finally, if C lies between A and D we have $b_1 = b + b_2$. Following the same line of reasoning, we then find

$$\cosh c = \cosh b \cosh a + \sinh a \sinh b \cdot \frac{\tanh b_2}{\tanh a}.$$

We now note that BCD is a hyperbolic triangle with a right angle at D and angle $\pi - \gamma$ at C. It follows from Lemma 1.2.7 that $-\cos\gamma = \cos(\pi - \gamma) = \frac{\tanh b_2}{\tanh a}$, so also in this case we obtain $\cosh b \cosh c - \sinh b \sinh c \cos\gamma$. The proof is complete. □

The Poincaré disk model

Starting from the Poincaré half plane model set up above, we will now construct a model for the hyperbolic plane in the (open) unit disk $\{z \in \mathbb{C} : |z| < 1\}$.

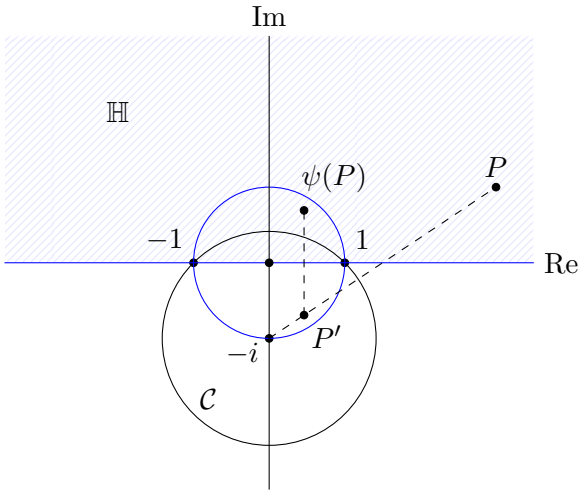

Figure 1.3: Construction of the Poincaré disk model. The map ψ is the composition of inversion in the circle $\mathcal{C}$ centered at $-i$ with radius $\sqrt{2}$ and reflection in the real axis. Under inversion in $\mathcal{C}$ the real axis maps to the unit circle. The point $P \in \mathbb{H}$ has inverse P' in $\mathcal{C}$ and image $\psi(P)$ under ψ. We have $\psi(P) \in \mathbb{D}$, where $\mathbb{D}$ is the open unit disk.

Let $\mathcal{C}$ denote the circle with center $-i$ that passes through 1 and -1 (Figure 1.3). The radius of $\mathcal{C}$ is $\sqrt{2}$. Let ψ denote the composition of inversion in $\mathcal{C}$ followed by reflection in the real axis.

Because the image of the real axis under inversion in $\mathcal{C}$ is the unit circle, the upper half plane $\mathbb{H}$ is mapped bijectively to the open unit disk $\mathbb{D} = \{z \in \mathbb{C} : |z| < 1\}$ by ψ (Figure 1.3). An explicit formula for ψ is given by $\psi(z) = \frac{iz+1}{z+i}$. Using ψ, we obtain a model for the hyperbolic plane in the unit disk. This model is called the Poincaré disk model. The hyperbolic distance between two points $a, b \in \mathbb{D}$ is defined as the hyperbolic distance between their preimages $\psi^{-1}(a)$, $\psi^{-1}(b) \in \mathbb{H}$.

Inversion maps circles and lines to circles and lines [8]. In particular, vertical lines in $\mathbb{H}$ are mapped to circle arcs in $\mathbb{D}$. Because vertical lines in $\mathbb{H}$ are perpendicular to the real axis (which is mapped to the boundary of $\mathbb{D}$ under the inversion) and inversion is angle-preserving [8], these circle arcs are perpendicular to the boundary of $\mathbb{D}$. The same holds for half circles in $\mathbb{H}$ centered at the real axis. We conclude that ψ maps hyperbolic lines to circle arcs in $\mathbb{D}$ perpendicular to the boundary of the disk. We have now found the geodesics in the Poincaré disk model.

Since inversion is angle-preserving, the hyperbolic trigonometric results from the previous section are still valid in this model of the hyperbolic plane. The inverse of ψ is given by $\psi^{-1} : z \mapsto \frac{-iz+1}{z-i}$. Therefore, we can naturally define the hyperbolic length of a path $\gamma : [0,1] \to \mathbb{D}$ as

$$\ell_{\mathbb{H}}(\psi^{-1} \circ \gamma) = \int_0^1 \frac{|(\psi^{-1} \circ \gamma)'(t)|}{\operatorname{Im} \psi^{-1} \circ \gamma(t)} \,\mathrm{d}t = \int_0^1 \frac{|(\psi^{-1})'(\gamma(t))||\gamma'(t)|}{\operatorname{Im} \psi^{-1} \circ \gamma(t)} \,\mathrm{d}t.$$

Since

$$(\psi^{-1})'(w) = \frac{-2}{(w-i)^2} \quad \text{and} \quad \operatorname{Im} \psi^{-1}(w) = \frac{1-|w|^2}{|i-w|^2},$$

we find

$$\ell_{\mathbb{H}}(\psi^{-1} \circ \gamma) = \int_0^1 \frac{|(\psi^{-1})'(\gamma(t))||\gamma'(t)|}{\operatorname{Im} \psi^{-1} \circ \gamma(t)} \,\mathrm{d}t = \int_0^1 \frac{2|\gamma'(t)|}{1-|\gamma(t)|^2} \,\mathrm{d}t.$$

We see that to compute distances in $\mathbb{D}$ we have to integrate $\frac{2}{1-|z|^2}$ instead of $\frac{1}{\operatorname{Im} z}$ along a path. We conclude that the metric on $\mathbb{D}$ induced by ψ is the metric induced by the differential form $\mathrm{d}s = \frac{2\,\mathrm{d}z}{1-|z|^2}$.

Lemma 1.2.10. *Let $0 \le x < 1$. The point x in the Poincaré disk model lies at hyperbolic distance $\log(\frac{1+x}{1-x})$ from the origin.*

Proof. Integrating over the path $\gamma : t \mapsto xt$ we find

$$d_{\mathbb{D}}(0,x) = \int_0^1 \frac{2x}{1-x^2t^2} \,\mathrm{d}t = 2 \operatorname{arctanh}(x) = 2 \log\left(\frac{1+x}{1-x}\right),$$

as required. □

The metric on $\mathbb{D}$ also allows us to define hyperbolic areas. We can define the hyperbolic area of a region $A \subset \mathbb{D}$ to be

$$\int_A \mathrm{d}s^2 = \int_A \frac{(2\,\mathrm{d}z)^2}{(1-|z|^2)^2}.$$

The proof of Lemma 1.2.11 shows how this formula can be used in computations.

Lemma 1.2.11. *A disk with hyperbolic radius r centered at the origin has circumference $2\pi \sinh(r)$ and area $2\pi(\cosh(r) - 1)$.*

Proof. A hyperbolic radius r corresponds to a Euclidean radius of $R = \frac{e^r-1}{e^r+1}$ by Lemma 1.2.10. We use the path $\gamma : t \mapsto Re^{2\pi ti}$ and obtain

$$\ell_{\mathbb{D}}(\gamma) = 2\int_0^1 \frac{2\pi R}{1-R^2} \,\mathrm{d}t = \frac{4\pi R}{1-R^2} = \frac{4\pi\left(\frac{e^r-1}{e^r+1}\right)}{1-\left(\frac{e^r-1}{e^r+1}\right)^2} = 2\pi \sinh(r)$$

for the circumference of the disk. For the area calculation, we first calculate the area of the disk with radius r intersected with the first quadrant. We call this region A, so $A = \{(Ru, Rv) : 0 \leq u, 0 \leq v, u^2 + v^2 \leq 1\}$. The area of A is given by

$$\begin{aligned}[A] &= \int_A \frac{(\,\mathrm{d}z)^2}{(1-|z|^2)^2} = \int_A \frac{\mathrm{d}x\,\mathrm{d}y}{(1-x^2-y^2)^2} \\ &= \int_0^1 \int_0^{\sqrt{1-u^2}} \frac{4R^2}{(1-(Ru)^2-(Rv)^2)^2}\,\mathrm{d}v\,\mathrm{d}u = \frac{\pi R^2}{(R^2-1)}.\end{aligned}$$

We now substitute $R = \frac{e^r-1}{e^r+1}$ to obtain

$$[A] = \frac{\pi R^2}{(R^2-1)} = \frac{\pi\left(\frac{e^r-1}{e^r+1}\right)^2}{\left(\frac{e^r-1}{e^r+1}\right)^2 - 1} = \frac{\pi(\cosh(r)-1)}{2}.$$

This means that the area of the complete disk is given by $2\pi(\cosh(r)-1)$, as required. □

1.3 Poisson point processes

In this section we develop some theory about Poisson point processes. For a more elaborate introduction, see the book by Kingman [18]. We restrict ourselves to finite measure spaces (i.e. measure spaces with finite total measure), because this is all we need for our applications. The extension to σ-finite measure spaces is straightforward.

Let (S, Σ) be a measurable space and assume that the diagonal $\Delta_S = \{(s, s) : s \in S\}$ is a measurable subset of $S \times S$ (endowed with the product measure). This assumption will allow us to distinguish individual points. For example, S might be a Borel measurable subset of d-dimensional Euclidean space $\mathbb{R}^d$ and Σ might consist of the Borel measurable subsets of S. In this case, it is easy to see that the diagonal is measurable.

Recall that if a random variable X follows a Poisson distribution with mean $\mu \in [0, \infty)$, then X takes nonnegative integer values and it holds that $\mathbb{P}(X = k) = e^{-\mu}\mu^k/k!$ for all $k \in \mathbb{Z}_{\geq 0}$.

Definition 1.3.1 (Poisson process)**.** A *Poisson process* on S is a random countable subset $\mathcal{P}$ of S that has the following two properties:

(i) if $A_1, \ldots, A_n$ are disjoint measurable subsets of S, the random variables $|\mathcal{P} \cap A_1|, \ldots, |\mathcal{P} \cap A_n|$ are independent;

(ii) there exists a function $\mu : \Sigma \to [0, \infty)$ such that if A is a measurable subset of S, then $|\mathcal{P} \cap A|$ follows a Poisson distribution with mean $\mu(A)$.

Lemma 1.3.2. *The function $\mu : \Sigma \to [0, \infty)$ in Definition 1.3.1 is a measure on S, called the* mean measure *of $\mathcal{P}$.*

Proof. First note that $\mu(\emptyset) = 0$, because $|\mathcal{P} \cap \emptyset|$ follows a Poisson distribution with mean 0 (this is the distribution concentrated on 0). If $A_1, A_2, \ldots \in \Sigma$ are disjoint measurable subsets of S then

$$\sum_{n\geq 1} \mu(A_n) = \sum_{n\geq 1} \mathbb{E}[|\mathcal{P} \cap A_n|] = \mathbb{E}\left[\sum_{n\geq 1} |\mathcal{P} \cap A_n|\right] = \mathbb{E}\left[\left|\mathcal{P} \cap \bigcup_{n\geq 1} A_n\right|\right] = \mu\left(\bigcup_{n\geq 1} A_n\right)$$

so μ is countably additive. We conclude that μ is a measure. □

If $S \subset \mathbb{R}^d$ is a Borel measurable set and $\mu(A) = \int_A f d\lambda$ for all measurable $A \subset S$ (where λ denotes Lebesgue measure), then we call f the *intensity function* of the Poisson process.

From Definition 1.3.1(i) we have that the random variables $|\mathcal{P} \cap A|$ and $|\mathcal{P} \cap B|$ are independent if A and B are disjoint. This is a special case of the following lemma.

Lemma 1.3.3. *Let $\mathcal{P}$ be a Poisson process on S with mean measure μ and let $A, B \subset S$ be measurable sets. Then* $\mathrm{Cov}(|\mathcal{P} \cap A|, |\mathcal{P} \cap B|) = \mu(A \cap B)$.

Proof. Note that $|\mathcal{P} \cap A| = |\mathcal{P} \cap (A \cap B)| + |\mathcal{P} \cap (A \setminus B)|$ and similarly $|\mathcal{P} \cap B| = |\mathcal{P} \cap (A \cap B)| + |\mathcal{P} \cap (B \setminus A)|$. By bilinearity of covariance we find

$$\begin{aligned}\mathrm{Cov}(|\mathcal{P} \cap A|, |\mathcal{P} \cap B|) = \mathrm{Cov}(|\mathcal{P} \cap (A \cap B)|, |\mathcal{P} \cap (A \cap B)|) + \mathrm{Cov}(|\mathcal{P} \cap (A \setminus B)|, |\mathcal{P} \cap (A \cap B)|) \\ + \mathrm{Cov}(|\mathcal{P} \cap (A \cap B)|, |\mathcal{P} \cap (B \setminus A)|) + \mathrm{Cov}(|\mathcal{P} \cap (A \setminus B)|, |\mathcal{P} \cap (B \setminus A)|).\end{aligned}$$

By independence, all terms except the first are nonzero. The first term equals $\mathrm{Var}(|\mathcal{P} \cap (A \cap B)|) = \mu(A \cap B)$ because $|\mathcal{P} \cap (A \cap B)|$ follows a Poisson distribution with mean $\mu(A \cap B)$. □

We next establish that for many finite measures μ on S there exists a Poisson process with mean measure μ. (Recall that a measure μ is called finite if $\mu(S) < \infty$.) A sufficient condition for the existence of the Poisson process turns out to be that μ is non-atomic in the sense that all singletons have measure 0, or, equivalently, that the diagonal has zero measure.

Lemma 1.3.4. *Let (S, Σ, μ) be a finite measure space (i.e. $\mu(S) < \infty$) such that Δ_S is measurable in $S \times S$. Then all singletons are measurable in S, and $\mu \times \mu(\Delta_S) = 0$ if and only if all singletons have measure* 0.

Proof. For any $s \in S$ the embedding $f_s : S \to S \times S$, $x \mapsto (s, x)$ is measurable. It follows that $\{s\} = f_s^{-1}(\Delta_S)$ is measurable. Suppose all singletons have measure 0. By Fubini's theorem, we then have

$$\mu \times \mu(\Delta_S) = \int_S \int_S \mathbf{1}_{\Delta_S}(x, y)\, \mathrm{d}\mu(x)\, \mathrm{d}\mu(y).$$

The inner integral equals $\mu(\{y\}) = 0$, so $\mu \times \mu(\Delta_S) = 0$. If conversely $\mu \times \mu(\Delta_S) = 0$, then we have $\mu(\{s\})^2 = \mu \times \mu(\{(s, s)\}) \leq \mu \times \mu(\Delta_S) = 0$ for all $s \in S$. □

In the case that $S \subset \mathbb{R}^d$ is Borel measurable and Σ is the corresponding Borel σ-algebra, this assumption will for example be satisfied if μ admits a density with respect to the Lebesgue measure. We now derive the existence of the Poisson process under the condition of Lemma 1.3.4.

Theorem 1.3.5 (Existence Theorem)**.** *Let μ be a finite measure on S (i.e. $\mu(S) < \infty$) such that $\mu \times \mu(\Delta_S) = 0$. Then there exists a Poisson process on S with μ as its mean measure.*

Proof. This is clear if $\mu(S) = 0$, so suppose $\mu(S) > 0$. Note that $p(A) = \mu(A)/\mu(S)$ defines a probability measure on S. We now endow the product $S^{\mathbb{N}}$ of (countably) infinitely many copies of (S, Σ, p) with the corresponding product measure $p^{\mathbb{N}}$ to make it into a probability space. An element of $S^{\mathbb{N}}$ has the form $(s_1, s_2, \ldots)$ where the s_i are points in S. We claim that with probability 1 all the s_i are distinct. From the assumption $\mu \times \mu(\Delta_S) = 0$ it follows that $p^{\mathbb{N}}(\{s_i = s_j\}) = 0$ for any two distinct indices i and j. Taking the countable union over all pairs i, j of distinct indices, we indeed find the desired result that with probability 1 all the s_i are distinct. We now define $\mathcal{P}$ as follows. Consider the measure space $(\mathbb{Z}_{\geq 0}, \wp(\mathbb{Z}_{\geq 0}), p_\mu)$, where $\wp(\mathbb{Z}_{\geq 0})$ denotes the power set of $\mathbb{Z}_{\geq 0}$ and p_μ defines a Poisson distribution with mean μ: $p_\mu(\{k\}) = e^{-\mu}\mu^k/k!$ for all $k \in \mathbb{Z}_{\geq 0}$. Let $(\Omega, \mathcal{F}, \mathbb{P})$ denote the product of $(\mathbb{Z}_{\geq 0}, \wp(\mathbb{Z}_{\geq 0}), p_\mu)$ and $(S^{\mathbb{N}}, \Sigma^{\mathbb{N}}, p^{\mathbb{N}})$ endowed with the product measure ($\Sigma^{\mathbb{N}}$ denotes the product σ-algebra on $S^{\mathbb{N}}$). An element of Ω has the form $\omega = (n(\omega), s_1(\omega), s_2(\omega), \ldots)$. For $\omega \in \Omega$, we now define the random set $\mathcal{P}(\omega) = \{s_1(\omega), \ldots, s_{n(\omega)}(\omega)\} \subset S$ (if $n(\omega) = 0$ this is

the empty set). With probability 1 the set $\mathcal{P}(\omega)$ is finite and has $|\mathcal{P}(\omega)| = n(\omega)$ elements (this holds if all s_i are distinct). We claim that $\mathcal{P} = \mathcal{P}(\omega)$ is the required Poisson process. Let $A \subset S$ be measurable and write $p = p(A) = \mu(A)/\mu(S)$. Now because $|\mathcal{P}|$ follows a Poisson distribution with mean $\mu(S)$, we can compute

$$\begin{aligned}\mathbb{P}(|\mathcal{P} \cap A| = k) &= \sum_{n \geq k} \mathbb{P}(|\mathcal{P} \cap A| = k \mid |\mathcal{P}| = n)\mathbb{P}(|\mathcal{P}| = n) \\ &= \sum_{n \geq k} \binom{n}{k} p^k (1-p)^{n-k} e^{-\mu(S)} \frac{\mu(S)^n}{n!} \\ &= e^{-\mu(S)} \frac{p^k \mu(S)^k}{k!} \sum_{n \geq k} \frac{((1-p)\mu(S))^{n-k}}{(n-k)!} = e^{-\mu(S)} \frac{(p\mu(S))^k}{k!}\end{aligned}$$

because $\sum_{n \geq k} \frac{((1-p)\mu(S))^{n-k}}{(n-k)!} = \sum_{\ell \geq 0} \frac{((1-p)\mu(S))^{\ell}}{(\ell)!} = e^{(1-p)\mu(S)}$. We conclude that $|\mathcal{P} \cap A|$ follows a Poisson distribution with mean $p\mu(S) = \mu(A)$. This proves condition (ii) of Definition 1.3.1. For condition (i), we consider disjoint mesaurable subsets $A_1, \ldots, A_n$ of S. Write $p_i = p(A_i)$ for $1 \leq i \leq n$ and let $p_0 = 1 - \sum_{i=1}^n p_i$. Consider nonnegative integers $k_1, \ldots, k_n$ with sum $k_1 + \ldots + k_n = k$. We have

$$\begin{aligned}\mathbb{P}\left(|\mathcal{P} \cap A_i| = k_i \text{ for } 1 \leq i \leq n\right) &= \sum_{m \geq k} \mathbb{P}(|\mathcal{P} \cap A_i| = k_i \text{ for } 1 \leq i \leq n \mid |\mathcal{P}| = m)\mathbb{P}(|\mathcal{P}| = m) \\ &= \sum_{m \geq k} \binom{m}{k_1, k_2, \ldots, k_n} \left(\prod_{i=1}^n p_i^{k_i}\right) p_0^{m-k} e^{-\mu(S)} \frac{\mu(S)^m}{m!} \\ &= e^{-\mu(S)} \left(\prod_{i=1}^n \frac{p_i^{k_i}}{k_i!}\right) \mu(S)^k \sum_{m \geq k} \frac{p_0^{m-k} \mu(S)^{m-k}}{(m-k)!} \\ &= e^{-\mu(S)} \left(\prod_{i=1}^n \frac{p_i^{k_i}}{k_i!}\right) \mu(S)^k e^{p_0 \mu(S)} \\ &= \prod_{i=1}^n \frac{(\mu(S)p_i)^{k_i}}{k_i!} e^{-\mu(S)p_i} = \prod_{i=1}^n \mathbb{P}(|\mathcal{P} \cap A_i| = k_i)\end{aligned}$$

because $|\mathcal{P} \cap A_i|$ follows a Poisson distribution with mean $\mu(A_i) = p_i\mu(S)$ for each i. This shows independence, so $\mathcal{P}$ satisfies both conditions in Definition 1.3.1. We conclude that $\mathcal{P}$ is the required Poisson process. □

We call two Poisson processes $\mathcal{P}_1$ and $\mathcal{P}_2$ on S *independent* if the random variables $|\mathcal{P}_1 \cap A|$ and $|\mathcal{P}_2 \cap B|$ are independent for any measurable $A, B \subset S$. The following result allows us to "add" independent Poisson processes. It can be seen as an extension of the standard result that the sum of two independent Poisson variables is again Poisson distributed.

Theorem 1.3.6 (Superposition Theorem)**.** *Let $\mathcal{P}_1$ and $\mathcal{P}_2$ be independent Poisson process on S with mean measures μ_1 and μ_2 respectively. If $\mu_1 \times \mu_2(\Delta_S) = 0$, then $\mathcal{P}_1 \cup \mathcal{P}_2$ is a Poisson process on S with mean measure $\mu_1 + \mu_2$.*

Proof. For measurable subsets C of $S \times S$ we define $M(C) = \mathbb{E}|\mathcal{P}_1 \times \mathcal{P}_2 \cap C|$. Clearly, M defines a measure on $S \times S$. For measurable $A, B \subset S$ we have, using independence of $\mathcal{P}_1$ and $\mathcal{P}_2$,

$$\begin{aligned}M(A \times B) &= \mathbb{E}|\mathcal{P}_1 \times \mathcal{P}_2 \cap A \times B| \\ &= \mathbb{E}|\mathcal{P}_1 \cap A||\mathcal{P}_2 \cap B| = \mathbb{E}|\mathcal{P}_1 \cap A|\mathbb{E}|\mathcal{P}_2 \cap B| = \mu_1(A)\mu_2(B) = \mu_1 \times \mu_2(A \times B).\end{aligned}$$

By uniqueness of measure extensions, it follows that $M = \mu_1 \times \mu_2$. In particular,

$$\mathbb{E}|\mathcal{P}_1 \cap \mathcal{P}_2| = \mathbb{E}|\mathcal{P}_1 \times \mathcal{P}_2 \cap \Delta_S| = M(\Delta_S) = \mu_1 \times \mu_2(S) = 0$$

so $\mathcal{P}_1$ and $\mathcal{P}_2$ are disjoint with probability 1. Let $A_1, \ldots, A_n$ be disjoint subsets of S. The $2n$ random variables $|\mathcal{P}_i \cap A_j|$ for $i \in \{1, 2\}$, $j \in \{1, 2, \ldots, n\}$ are all independent, so the same holds for the random variables $|(\mathcal{P}_1 \cup \mathcal{P}_2) \cap A_j| = |\mathcal{P}_1 \cap A_j| + |\mathcal{P}_2 \cap A_j|$ for $j \in \{1, 2, \ldots, n\}$. Similarly, for measurable $A \subset S$ we know that $|(\mathcal{P}_1 \cup \mathcal{P}_2) \cap A| = |\mathcal{P}_1 \cap A| + |\mathcal{P}_2 \cap A|$ is the sum of independent Poisson distributed variables with means $\mu_1(A)$ and $\mu_2(A)$, respectively. We see that $|(\mathcal{P}_1 \cup \mathcal{P}_2) \cap A|$ follows a Poisson distribution with mean $\mu(A) = \mu_1(A) + \mu_2(A)$, so $\mathcal{P}_1 \cup \mathcal{P}_2$ indeed is a Poisson process with mean measure $\mu_1 + \mu_2$. □

The final result we prove allows us to transfer a Poisson process from one space to another (Theorem 1.3.8). Let S and T be measure spaces whose diagonals are measurable and let $f : S \to T$ be a measurable function. If μ is a measure on S, then $\mu^*(A) = \mu(f^{-1}(A))$ defines a measure on T, called the induced measure.

We will need the following elementary lemma.

Lemma 1.3.7. *The induced measure $(\mu \times \mu)^*$ of the product measure $\mu \times \mu$ on $S \times S$ under the map $f^\times : S \times S \to T \times T$, $f^\times : (s, s') \mapsto (f(s), f(s'))$ coincides with the product measure $\mu^* \times \mu^*$.*

Proof. By uniqueness of extended measures, it suffices to show that $(\mu \times \mu)^* = \mu^* \times \mu^*$ on all subsets of $T \times T$ of the form $A \times B$ with A, B measurable subsets of T. For such sets we have

$$\begin{aligned}(\mu \times \mu)^*(A \times B) &= \mu \times \mu((f^\times)^{-1}(A \times B)) = \mu \times \mu(f^{-1}(A) \times f^{-1}(B)) = \mu(f^{-1}(A))\mu(f^{-1}(B)) \\ &= \mu^*(A)\mu^*(B) = \mu^* \times \mu^*(A \times B),\end{aligned}$$

as required. □

Theorem 1.3.8 (Mapping Theorem)**.** *Let $\mathcal{P}$ be a Poisson process on S with mean measure μ. Suppose $f : S \to T$ is a measurable function and let μ^* be the induced measure. Assume that $\mu^* \times \mu^*(\Delta_T) = 0$, where $\Delta_T = \{(t, t) : t \in T\}$ is the diagonal of $T \times T$. Then $f(\mathcal{P})$ defines a Poisson process on T with μ^* as its mean measure.*

Proof. If f is injective on $\mathcal{P}$ we have $|f(\mathcal{P}) \cap A| = |\mathcal{P} \cap f^{-1}(A)|$ for all measurable $A \subset T$, from which the conclusion immediately follows. It therefore suffices to show that f is injective on $\mathcal{P}$ with probability 1. Write $F = \{(s_1, s_2) \in S \times S : f(s_1) = f(s_2)\} = (f^\times)^{-1}(\Delta_T)$, where $f^\times$ is defined as in Lemma 1.3.7. Applying this Lemma yields that $\mu \times \mu(F) = (\mu \times \mu)^*(\Delta_T) = \mu^* \times \mu^*(\Delta_T) = 0$. Write $\Delta_\mathcal{P} = \{(p, p) : p \in \mathcal{P}\}$ for the diagonal of $\mathcal{P} \times \mathcal{P}$. For measurable subsets C of $S \times S$ we define $M(C) = \mathbb{E}\left[|(\mathcal{P} \times \mathcal{P} \setminus \Delta_\mathcal{P}) \cap C|\right]$ as the expected number of pairs of points $(p, q) \in \mathcal{P} \times \mathcal{P}$ with $p \neq q$ that lie in C. It is clear that M defines a measure on $S \times S$. For measurable subsets A, B of S we have

$$\begin{aligned}M(A \times B) &= \mathbb{E}\left[|(\mathcal{P} \times \mathcal{P} \setminus \Delta_P) \cap (A \times B)|\right] \\ &= \mathbb{E}\left[|(\mathcal{P} \times \mathcal{P}) \cap (A \times B)|\right] - \mathbb{E}\left[|\Delta_\mathcal{P} \cap (A \times B)|\right] \\ &= \mathbb{E}\left[|(\mathcal{P} \cap A) \times (\mathcal{P} \cap B)|\right] - \mathbb{E}\left[|\mathcal{P} \cap (A \cap B)|\right] \\ &= \mathrm{Cov}(|\mathcal{P} \cap A|, |\mathcal{P} \cap B|) + \mathbb{E}\left[|\mathcal{P} \cap A|\right]\mathbb{E}\left[|\mathcal{P} \cap B|\right] - \mathbb{E}\left[|\mathcal{P} \cap (A \cap B)|\right] \\ &= \mu(A \cap B) + \mu(A)\mu(B) - \mu(A \cap B) = \mu(A)\mu(B) = \mu \times \mu(A \times B),\end{aligned}$$

where we used Lemma 1.3.3 to compute the covariance. It follows that the measures M and $\mu \times \mu$ coincide on all sets of the form $A \times B$ with $A, B \subset S$ measurable. By uniqueness of extended measures, these measures coincide. We find $M(F) = \mu \times \mu(F) = 0$, hence

$$\mathbb{E}\left[|\{p, q \in \mathcal{P} : p \neq q, f(p) = f(q)\}|\right] = \mathbb{E}\left[|(\mathcal{P} \times \mathcal{P} \setminus \Delta_\mathcal{P}) \cap \{(s_1, s_2) \in S \times S : f(s_1) = f(s_2)\}|\right] = 0.$$

It follows that f is injective on $\mathcal{P}$ with probability 1, as required. □

2

Hyperbolic random graphs

This chapter starts with the introduction of the KPKVB model (Section 2.1), which is the random graph model that this thesis is about. After defining the model, we also summarize its known properties. Next, in Section 2.2 we present some bounds on relevant parameters in the KPKVB model. In Section 2.3 we define a second random geometric graph model, this time in Euclidean space, that can be used as an approximation for the KPKVB model.

2.1 The KPKVB model

We study a specific model for random geometric graphs in the hyperbolic plane that we refer to as the Krioukov-Papadopoulos-Kitsak-Vahdat-Boguñá model or KPKVB model, after its authors [21]. In this section we describe the construction of this random graph.

The model is denoted by $\mathcal{G}(N;\alpha,\nu)$. Here N denotes the number of vertices and $\alpha,\nu>0$ are fixed parameters. We think of N as "large"; later we study the asymptotic behavior of the graph as N tends to infinity. The construction starts by setting $R=2\log(N/\nu)$. The vertex set of the graph will be a set of N points inside the disk $\mathcal{D}_R$ with radius R centered at the origin in the hyperbolic plane (we work in the Poincaré disk model). The N points are sampled independently according to the probability density function

$$f(r,\vartheta)=\frac{1}{2\pi}\frac{\alpha\sinh(\alpha r)}{\cosh(\alpha R)-1} \qquad (r\in[0,R],\vartheta\in(-\pi,\pi]).$$

Here (r,ϑ) denote the polar coordinates of a point in the hyperbolic plane, so r denotes the (hyperbolic) distance to the origin and ϑ denotes the angle with the positive x-axis in the Poincaré disk representation. Equivalently, ϑ and r are sampled independently from the uniform distribution on $(-\pi,\pi]$ and the distribution on $[0,R]$ determined by the probability density function $f(r)=\frac{\alpha\sinh(\alpha r)}{\cosh(\alpha R)-1}$, respectively. For $\alpha=1$ the resulting distribution is the uniform distribution on $\mathcal{D}_R$ (this follows from Lemma 1.2.11). For $\alpha<1$ there is a bias towards the center of the disk; for $\alpha>1$ there is a bias towards the periphery of the disk. We refer to the resulting distribution on $\mathcal{D}_R$ as the (α,R)-quasi uniform distribution.

The random set of N points serves as the vertex set of our graph. We connect a pair of vertices by an edge if and only if their hyperbolic distance is at most R. This means for example that if the origin O were to be one of the chosen points, then it would be connected to all other vertices of the graph.

The motivation behind this hyperbolic random graph model is that it has some of the properties of complex networks discussed in Section 1.1. As explained in Section 1.2, that these properties arise has to do with the fact that length and area increase exponentially in the hyperbolic plane. The inventors of the KPKVB model have used their model to study a variety of real-world networks, including the internet [5] and the world trade network [13]. The model has also been used to link complex networks to theoretical cosmology [20].

In our proofs, we will also consider a Poissonized variant of the model, in which the number of vertices is not fixed but sampled from a Poisson distribution with mean N. The vertex set of the graph then can be interpreted as the point set of a Poisson process on $\mathcal{D}_R$ with intensity function $Nf(r,\vartheta)$. The advantage of this approach is that what happens in disjoint subsets of

$\mathcal{D}_R$ is now independent (this is not the case in the original model, because if we know in the original model that the upper half of the disk contains N points, we can be sure that the lower half does not contain any points). The connection rule in the Poissonized model, which is denoted by $\mathcal{G}_{\mathrm{Po}}(N;\alpha,\nu)$, is the same as in the original model. The following Lemma shows that if an event happens a.a.s. in the Poissonized model, it also happens a.a.s. in the original model, provided the probability of the event approaches 1 sufficiently fast in the Poissonized model.

Lemma 2.1.1. *Let X be an event that happens with probability $1-O(N^{-1})$ in $\mathcal{G}_{\mathrm{Po}}(N;\alpha,\nu)$. Then X happens a.a.s. in $\mathcal{G}(N;\alpha,\nu)$.*

Proof. Let Z denote the number of vertices of G_{Po}. Then $Z \sim \mathrm{Po}(N)$. We find

$$\mathbb{P}(Z=N) = \frac{N^N e^{-N}}{N!} = \left(\frac{N}{e}\right)^N (N!)^{-1} \sim \frac{1}{\sqrt{2\pi N}}$$

by Stirling's approximation [10, p. 37], so $\mathbb{P}(Z=N) = \Theta(N^{-\frac{1}{2}})$. Furthermore, we see that $\mathcal{G}(N;\alpha,\nu)$ is obtained when $\mathcal{G}_{\mathrm{Po}}(N;\alpha,\nu)$ is conditioned on $Z=N$. We compute

$$\mathbb{P}(X^c \mid Z=N) \leq \frac{\mathbb{P}(X^c)}{\mathbb{P}(Z=N)} = \frac{O(N^{-1})}{\Theta(N^{-\frac{1}{2}})} = O(N^{-\frac{1}{2}}) = o(1),$$

so X happens a.a.s. when conditioned on $Z=N$. □

We continue by summarizing some of the known properties of the KPKVB model. The KPKVB model was rigorously studied first by Gugelmann et al. [14]. The usual approach is to study the asymptotic behavior of the graph for $N \to \infty$ for a fixed choice of the parameters α and ν. The original model of Krioukov et al. [21] also included a third parameter ζ, which controls the curvature of the hyperbolic plane on which the graph lives. Our setup corresponds to $\zeta = 1$, which can be chosen without any loss of generality [3]. We also remark that some authors (e.g. [14]) use $C = -2\log(\nu)$ as a parameter instead of ν.

What we will see below is that the behavior of the random graph depends strongly on the values of α and ν. There are roughly three regimes with different behavior: these regimes correspond to values of α that are in $(0,\frac{1}{2})$, $(\frac{1}{2},1)$ and $(1,\infty)$, respectively. What happens at the critical values of $\alpha=\frac{1}{2}$ and $\alpha=1$ is found to depend on ν.

Figure 2.1 shows examples of KPKVB random graphs for different values of α.

The degree sequence

The shape of the degree sequence depends on α. For $\alpha < \frac{1}{2}$ the average degree is not bounded, but increases with N (see Corollary 2.2.5 below). However, for $\alpha > \frac{1}{2}$ the average degree is bounded. Gugelmann et al. [14] prove the following results:

- for $\alpha > \frac{1}{2}$, the degree sequence is a power law with exponent $2\alpha+1$;
- the (expected) average degree of $\mathcal{G}(N;\alpha,\nu)$ approaches a limit that is proportional to ν.

In the original paper, Krioukov et al. [21] already provided heuristic arguments for the fact that the degree sequence is a power law.

We see that by choosing the α and ν parameters of the model, one gains control over the degree sequence. The power law exponent can be tuned to any number > 2 by choosing the α parameter and the average degree can be tuned to any number by choosing the ν parameter. Because in real-world networks power-law exponents are usually found between 2 and 3, in the study of KPKVB random graphs values of α between $\frac{1}{2}$ and 1 have received the most interest.

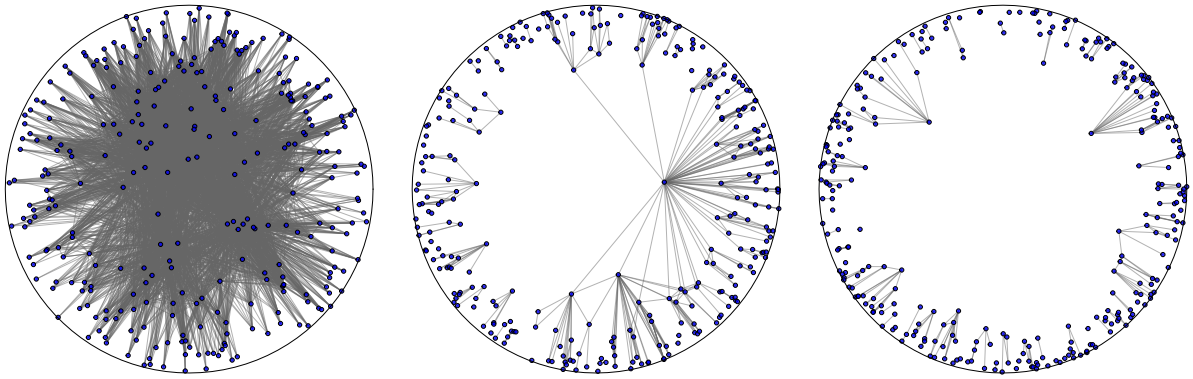

Figure 2.1: Computer simulations of the KPKVB model for different values of α. Graphs are drawn in the native representation of the hyperbolic plane, in which hyperbolic polar coordinates (r, ϑ) are interpreted as if they were Euclidean polar coordinates. Parameters used: $N = 300$, $\nu = 1$, $\alpha = 0.3$ (left), $\alpha = 0.8$ (center), $\alpha = 1.3$ (right).

Connectivity

The results on the degree sequence imply that for $\alpha > \frac{1}{2}$ the graph $\mathcal{G}(N; \alpha, \nu)$ is disconnected a.a.s., because there will be isolated vertices. For $\alpha < \frac{1}{2}$ it is however easy to prove that $\mathcal{G}(N; \alpha, \nu)$ is connected [4]. This is done by showing that a.a.s. there is a connected set of 8 vertices close to the origin such that each vertex of the graph is connected to one of these 8 vertices. Furthermore, Bode et al. [4] study the connectivity at the critical value of $\alpha = \frac{1}{2}$ and show that the probability that the graph is connected tends to a limit $f(\nu)$. They also prove that f is a continuous function of ν that has limit 0 for $\nu \to 0$, is strictly increasing on $(0, \pi)$ and is equal to 1 for $\nu \geq \pi$ [4].

Component structure

For values of $\alpha > \frac{1}{2}$, for which $\mathcal{G}(N; \alpha, \nu)$ is a.a.s. disconnected, it makes sense to study the component structure of $\mathcal{G}(N; \alpha, \nu)$. In doing so, it turns out that there is another phase transition at $\alpha = 1$. Bode et al. [3] study the size of the largest component. For $\alpha > 1$ the size $|L_1|$ of the largest component is sublinear in N, which means that a.a.s. we have $|L_1| = o(N)$ [3]. For $\alpha < 1$ however, the largest component is linear in N: we have $|L_1| = \Omega(N)$ a.a.s.. Because the second largest component is sublinear [19], the largest component could for $\alpha \in (\frac{1}{2}, 1)$ be called the *giant component*. At $\alpha = 1$ the existence of a linear component depends on the value of ν [3].

Fountoulakis and Müller [11] study the size of the largest component in more detail. They show that for any α, ν there exists a $c = c(\nu, \alpha)$ such that $|L_1|/N \to c$ in probability as $N \to \infty$. This is referred to as a law of large numbers for the largest component. For $\alpha \leq \frac{1}{2}$ it turns out that $c = 1$ [11]. For $\alpha > 1$ it was already known that $c = 0$, whereas for $\alpha < 1$ it is positive [3]. At $\alpha = 1$ it depends on ν whether c is positive. It turns out that there exists a critical value ν_{crit} such that $c = 0$ for $\nu < \nu_{\text{crit}}$ but $c > 0$ for $\nu > \nu_{\text{crit}}$ [11]. Fountoulakis and Müller [11] further show that c is decreasing in α and increasing in ν.

Distances

Kiwi and Mitsche [19] study the diameter in the KPKVB model for $\alpha \in (\frac{1}{2}, 1)$. They prove a polylogarithmic upper bound, i.e. an upper bound that is a polynomial in $\log N$, for the diameter

of each component that holds a.a.s.. As a complementary result, they show that a.a.s. there are components of diameter $\Omega(\log N)$ [19]. The results of Kiwi and Mitsche are improved by Friedrich and Krohmer [12], who show that a.a.s. the giant component has diameter $\Omega(\log N)$. Furthermore, they improve the exponent in the polylogarithmic upper bound [12]. In both cases, the lower bounds on the diameter are proven by showing that there are induced paths of logarithmic length close to the boundary of the disk. The upper bounds are proven by finding short paths between vertices. The work by Friedrich and Krohmer [12] shows that there is an "inner core" of diameter $O(\log \log N)$ which consists of all vertices at distance at least $\Theta(\log R)$ from the boundary. However, their results leave open the possibility that some vertices are at polylogarithmic distance from the inner core.

In this work, we show that for $\alpha \in (\frac{1}{2}, 1)$ the diameter of the giant component is in fact logarithmic in the number of vertices, by proving a logarithmic upper bound that holds a.a.s.. Our upper bound also holds for the other components of the graph. For $\alpha = 1$ and ν sufficiently large we also prove a logarithmic upper bound. We do not discuss the case $\alpha > 1$ (or $\alpha = 1$ and small ν), for which the giant component disappears. For $\alpha < \frac{1}{2}$ it follows from [4] that the graph is a.a.s. connected and has diameter at most 3.

Instead of looking at maximum distances, Abdullah et al. [1] consider typical distances. They show that for $\alpha \in (\frac{1}{2}, 1)$ the distance between two randomly chosen vertices in the same component is of the order $\log \log N$. In the terminology of [26], this means that KPKVB random graphs are "ultra-small networks".

2.2 Some estimates

In this section we use the results of Section 1.2 to give bounds on relevant quantities in the KPKVB model. The estimates below can for instance be used to determine whether two vertices are connected (Lemma 2.2.3) or what the expected degree of a vertex is (Lemma 2.2.4).

Recall that the (α, R)-quasi uniform distribution has density $f(r, \vartheta) = \frac{\alpha \sinh(\alpha r)}{2\pi(\cosh(\alpha R)-1)}$, where $\int_{\mathcal{D}_R} f = 1$. The expected number of vertices of $G = G(N; \alpha, \nu)$ and $G_{\mathrm{Po}} = G_{\mathrm{Po}}(N; \alpha, \nu)$ in a subregion $A \subset \mathcal{D}_R$ equals $N\mu(A)$, where $\mu(A) = \int_A f$. The number of vertices of G_{Po} in A follows a Poisson distribution with mean $N\mu(A)$.

We first give bounds for the total density of a disk centered at the origin. By $B_u(x)$ we denote the disk in the hyperbolic plane with center u and hyperbolic radius x.

Lemma 2.2.1. *For $0 \le x \le R$ we have*

$$(1 - e^{-\alpha x})^2 e^{-\alpha(R-x)} \le \mu(B_0(x)) \le e^{-\alpha(R-x)}.$$

Proof. Note that

$$\begin{aligned}
\mu(B_0(x)) &= \int_0^{2\pi} \int_0^x f(y)\,\mathrm{d}y\,\mathrm{d}\vartheta = \int_0^x \frac{\alpha \sinh(\alpha y)}{\cosh(\alpha R) - 1}\,\mathrm{d}y \\
&= \frac{\cosh(\alpha x) - 1}{\cosh(\alpha R) - 1} = \frac{e^{\alpha x} + e^{-\alpha x} - 2}{e^{\alpha R} + e^{-\alpha R} - 2} = \frac{e^{\alpha x}}{e^{\alpha R}} \cdot \left(\frac{1 - e^{-\alpha x}}{1 - e^{-\alpha R}}\right)^2 \\
&= e^{-\alpha(R-x)} \cdot \left(\frac{1 - e^{-\alpha x}}{1 - e^{-\alpha R}}\right)^2.
\end{aligned}$$

Because $x \le R$ we have $\frac{1-e^{-\alpha x}}{1-e^{-\alpha R}} \le 1$. This proves the upper bound. The lower bound follows from the fact that $1 - e^{-\alpha R} \le 1$. □

Lemma 2.2.1 can be used to show that for $\alpha > \frac{1}{2}$, a.a.s. there are no vertices close to the origin.

Lemma 2.2.2. *Let $\alpha > \frac{1}{2}$ and write $\varepsilon = \frac{1}{2}(1 - \frac{1}{2\alpha})$. A.a.s., there are no vertices of G_{Po} or G in $B_0(\varepsilon R)$.*

Proof. Using Lemma 2.2.1 we estimate that the expected number of vertices in $B_0(\varepsilon R)$ is

$$N\mu(B_0(\varepsilon R)) \leq \nu e^{R/2} e^{-\alpha(R-\varepsilon R)} = O(e^{R(\frac{1}{2}-\alpha+\alpha\varepsilon)}) = o(1),$$

because $\frac{1}{2} - \alpha + \alpha\varepsilon = \frac{1}{2} - \alpha + \alpha(\frac{1}{2} - \frac{1}{4\alpha}) = \frac{1}{4} - \frac{1}{2}\alpha < 0$. (Note that in the asymptotics above, the implicit constant may depend on ν.) □

We now consider the connection rule of G. Recall that two points (r_1, ϑ_1) and (r_2, ϑ_2) in $\mathcal{D}_R$ are connected by an edge in the KPKVB model if and only if their hyperbolic distance is at most R. Let $\vartheta(r_1, r_2) \in [0, \pi]$ denote the maximal value of φ such that two points with radial coordinates r_1 and r_2 and angular distance φ are connected. Then (r_1, ϑ_1) and (r_2, ϑ_2) are connected by an edge if and only if $|\vartheta_1 - \vartheta_2|_{2\pi} \leq \vartheta(r_1, r_2)$. Note that if $r_1 + r_2 \leq R$ we have $\vartheta(r_1, r_2) = \pi$ because (r_1, ϑ_1) and (r_2, ϑ_2) are always connected by the triangle inequality. Therefore, we assume that $r_1 + r_2 > R$.

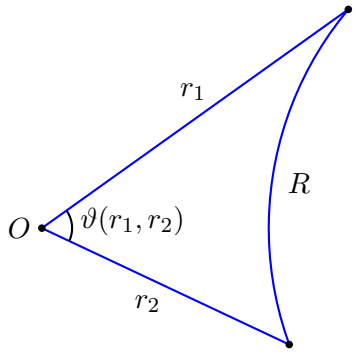

Figure 2.2: Using the hyperbolic cosine rule.

Note that $\vartheta(r_1, r_2)$ is the angle opposite to R in a hyperbolic triangle with side lengths r_1, r_2 and R (Figure 2.2). We can therefore use the hyperbolic cosine rule (Theorem 1.2.9) to compute $\vartheta(r_1, r_2)$. The following lemma, which is similar to Lemma 27 in [11], gives us sharp bounds for the resulting expression. We need the assumption that r_1/R and r_2/R are bounded away from 0, which can usually be guaranteed by Lemma 2.2.2.

Lemma 2.2.3. *Let $\gamma > 0$. There exists a constant $K > 0$ such that for all sufficiently large R and $r_1, r_2 \in [0, R]$ satisfying $r_1 + r_2 > R$ and $\min(r_1, r_2) \geq \gamma R$, we have*

$$2e^{\frac{1}{2}(R-r_1-r_2)} - Ke^{\frac{1}{2}(-R-3\min(r_1,r_2)+\max(r_1,r_2))} \leq \vartheta(r_1, r_2) \leq 2e^{\frac{1}{2}(R-r_1-r_2)} + 3e^{\frac{3}{2}(R-r_1-r_2)}.$$

As a consequence, we also have the weaker bounds $\vartheta(r_1, r_2) = \Theta(e^{\frac{1}{2}(R-r_1-r_2)})$ and $\vartheta(r_1, r_2) = 2e^{\frac{1}{2}(R-r_1-r_2)} \pm O(e^{R-r_1-r_2})$.

Proof. By the hyperbolic cosine rule, we have

$$\begin{aligned}\cos(\vartheta(r_1, r_2)) &= \frac{\cosh(r_1)\cosh(r_2) - \cosh(R)}{\sinh(r_1)\sinh(r_2)} \\ &= 1 + 2 \cdot \frac{e^{-2r_1} + e^{-2r_2} - e^{R-r_1-r_2} - e^{-R-r_1-r_2}}{(1 - e^{-2r_1})(1 - e^{-2r_2})}.\end{aligned}$$

Because $(e^{-r_1} - e^{-r_2})^2 \geq 0$, we have

$$e^{-2r_1} + e^{-2r_2} \geq 2e^{-r_1-r_2} \geq e^{-R-r_1-r_2} + e^{-2r_1-2r_2} = e^{-R-r_1-r_2}(1 + e^{R-r_1-r_2}).$$

Multiplying by $1 - e^{R-r_1-r_2} \geq 0$, it follows that

$$\begin{aligned}(e^{-2r_1} + e^{-2r_2})(1 - e^{R-r_1-r_2}) &\geq e^{-R-r_1-r_2}(1 + e^{R-r_1-r_2})(1 - e^{R-r_1-r_2}) \\ &= e^{-R-r_1-r_2} - e^{R-3r_1-3r_2},\end{aligned}$$

or, equivalently,

$$e^{-2r_1} + e^{-2r_2} - e^{R-3r_1-r_2} - e^{R-r_1-3r_2} \geq e^{-R-r_1-r_2} - e^{R-3r_1-3r_2}.$$

Adding $e^{R-r_1-r_2} + e^{R-3r_1-3r_2} - e^{-2r_1} - e^{-2r_2}$ to both sides, this rewrites to

$$e^{R-r_1-r_2}(1 - e^{-2r_1})(1 - e^{-2r_2}) \geq e^{R-r_1-r_2} + e^{-R-r_1-r_2} - e^{-2r_1} - e^{-2r_2}.$$

We divide both sides by $-(1 - e^{-2r_1})(1 - e^{-2r_2}) < 0$ to obtain

$$-e^{R-r_1-r_2} \leq \frac{e^{-2r_1} + e^{-2r_2} - e^{R-r_1-r_2} - e^{-R-r_1-r_2}}{(1 - e^{-2r_1})(1 - e^{-2r_2})}.$$

It follows that

$$1 - 2e^{R-r_1-r_2} \leq 1 + 2 \cdot \frac{e^{-2r_1} + e^{-2r_2} - e^{R-r_1-r_2} - e^{-R-r_1-r_2}}{(1 - e^{-2r_1})(1 - e^{-2r_2})} = \cos(\vartheta(r_1, r_2))$$

Since $\cos(t) \leq 1 - \frac{2t^2}{\pi^2}$ on $[0, \pi]$, it follows that

$$1 - 2e^{R-r_1-r_2} \leq \cos(\vartheta(r_1, r_2)) \leq 1 - \frac{2\vartheta(r_1, r_2)^2}{\pi^2},$$

implying $\vartheta(r_1, r_2) \leq \pi e^{\frac{1}{2}(R-r_1-r_2)}$. Now, by $\cos(t) \leq 1 - \frac{t^2}{2} + \frac{t^4}{24}$ we also have

$$1 - 2e^{R-r_1-r_2} \leq \cos(\vartheta(r_1, r_2)) \leq 1 - \frac{\vartheta(r_1, r_2)^2}{2} + \frac{\vartheta(r_1, r_2)^4}{24}.$$

It follows (using $\pi^4 < 144$) that

$$\vartheta(r_1, r_2)^2 \leq 4e^{R-r_1-r_2} + \frac{\vartheta(r_1, r_2)^4}{12} \leq 4e^{R-r_1-r_2} + \frac{\pi^4}{12} e^{2(R-r_1-r_2)} \leq \left(2e^{\frac{1}{2}(R-r_1-r_2)} + 3e^{\frac{3}{2}(R-r_1-r_2)}\right)^2.$$

This concludes the proof of the upper bound.

For the lower bound, we note that since r_1 and r_2 are bounded away from 0 by $r_1, r_2 \geq \gamma R$, we have

$$\frac{1}{1 - e^{-2r_1}} = 1 + O(e^{-2r_1}) \qquad \text{and} \qquad \frac{1}{1 - e^{-2r_2}} = 1 + O(e^{-2r_2}).$$

It follows that

$$\begin{aligned}\cos(\vartheta(r_1, r_2)) &= 1 + 2 \cdot \frac{e^{-2r_1} + e^{-2r_2} - e^{R-r_1-r_2} - e^{-R-r_1-r_2}}{(1 - e^{-2r_1})(1 - e^{-2r_2})} \\ &= 1 + 2(e^{-2r_1} + e^{-2r_2} - e^{R-r_1-r_2} - e^{-R-r_1-r_2})(1 + O(e^{-2r_1}))(1 + O(e^{-2r_2})) \\ &= 1 + 2(e^{-2r_1} + e^{-2r_2} - e^{R-r_1-r_2} - e^{-R-r_1-r_2})(1 + O(e^{-2r_1}) + O(e^{-2r_2})) \\ &= 1 - 2e^{R-r_1-r_2} + O(e^{-2r_1}) + O(e^{-2r_2}) = 1 - 2e^{R-r_1-r_2} + O(e^{-2\min(r_1,r_2)}).\end{aligned}$$

By the inequality $\cos(t) \geq 1 - \frac{t^2}{2}$ (or, equivalently, $t^2 \geq 2(1-\cos(t))$) we find

$$\vartheta(r_1, r_2)^2 \geq 4e^{R-r_1-r_2} - O(e^{-2\min(r_1,r_2)}),$$

hence for some constant $L > 0$ we have $\vartheta(r_1, r_2)^2 \geq 4e^{R-r_1-r_2} - Le^{-2\min(r_1,r_2)}$. Take K such that $4K = L + 1$. Because $-r_1 - r_2 - 3\min(r_1, r_2) + \max(r_1, r_2) = -4\min(r_1, r_2)$, we have

$$Le^{\frac{1}{2}(-r_1-r_2-3\min(r_1,r_2)+\max(r_1,r_2))} = Le^{-2\min(r_1,r_2)}.$$

Furthermore, the inequality

$$e^{\frac{1}{2}(-r_1-r_2-3\min(r_1,r_2)+\max(r_1,r_2))} \geq K^2 e^{-R-3\min(r_1,r_2)+\max(r_1,r_2)}$$

holds for sufficiently large R. Indeed, the ratio between the right hand side and the left hand side is $K^2 e^{-R-\min(r_1,r_2)+\max(r_1,r_2)} \leq K^2 e^{-R-\gamma R+R} = K^2 e^{-\gamma R}$ which is ≤ 1 for sufficiently large R. Adding these two inequalities yields (using $4K = L + 1$)

$$4Ke^{\frac{1}{2}(-r_1-r_2-3\min(r_1,r_2)+\max(r_1,r_2))} \geq Le^{-2\min(r_1,r_2)} + K^2 e^{-R-3\min(r_1,r_2)+\max(r_1,r_2)}$$

for sufficiently large R. It follows that

$$\vartheta(r_1, r_2)^2 \geq 4e^{R-r_1-r_2} - Le^{-2\min(r_1,r_2)} \geq \left(2e^{\frac{1}{2}(R-r_1-r_2)} - Ke^{\frac{1}{2}(-R-3\min(r_1,r_2)+\max(r_1,r_2))}\right)^2.$$

The required conclusion now follows by taking square roots. □

For a point $u \in \mathcal{D}_R$ the set of points in $\mathcal{D}_R$ that lie at hyperbolic distance at most R from u is given by $B_0(R) \cap B_u(R)$. If u is a vertex of G, then another vertex is a neighbor of u if and only if it lies inside $B_0(R) \cap B_u(R)$. The following lemma gives rough bounds for the area of this set. It can be used to estimate the degree of u.

Lemma 2.2.4. *Let $\alpha > \frac{1}{2}$. Suppose $u \in \mathcal{D}_R$ lies at distance x from the origin. Then we have $\mu(B_0(R) \cap B_u(R)) = \Theta(e^{-x/2})$.*

Proof. From Lemma 2.2.3 we have $\vartheta(r_1, r_2) = \Theta(e^{(R-r_1-r_2)/2})$. Furthermore, we have

$$f(r, \vartheta) = \frac{\alpha \sinh(\alpha r)}{2\pi(\cosh(\alpha R) - 1)} = \Theta(e^{\alpha(r-R)}).$$

We now compute

$$\begin{aligned}
\mu(B_0(R) \cap B_u(R)) &= \int_0^R \int_{-\vartheta(x,r)}^{\vartheta(x,r)} f(r, \vartheta)\, \mathrm{d}\vartheta\, \mathrm{d}r \\
&= \Theta\left(\int_0^R e^{(R-r-x)/2} e^{\alpha(r-R)}\, \mathrm{d}r\right) \\
&= \Theta\left(e^{-x/2} e^{R(\frac{1}{2}-\alpha)} \int_0^R e^{-r(\frac{1}{2}-\alpha)}\, \mathrm{d}r\right) \\
&= \Theta\left(e^{-x/2} e^{R(\frac{1}{2}-\alpha)} e^{-R(\frac{1}{2}-\alpha)}\right) = \Theta(e^{-x/2}),
\end{aligned}$$

as required. □

Corollary 2.2.5. *For $\alpha < \frac{1}{2}$, the expected degree of a random chosen vertex of $\mathcal{G}(N; \alpha, \nu)$ is $\Omega(\log N)$.*

Proof. We use Lemma 2.2.4. The radial coordinate y of a point chosen according to the (α, R)-quasi uniform distribution is a random variable with density $f(y) = \mathbf{1}_{[0,R]} \frac{\alpha \sinh(\alpha y)}{\cosh(\alpha R)-1} = \mathbf{1}_{[0,R]} \Theta(e^{\alpha(y-R)})$. It follows that the expected degree of a vertex equals

$$\int_0^R \Theta(e^{\alpha(y-R)})\Theta(Ne^{-y/2})\,\mathrm{d}y = \Theta\left(\int_0^R e^{(\alpha-\frac{1}{2})(y-R)}\,\mathrm{d}y\right) = \Omega(R)$$

(the integrand is at least 1 because $(\alpha - \frac{1}{2})(y-R) > 0$), as required. □

2.3 The idealized model

In this section we will construct a random graph model that behaves similarly to the KPKVB model but is more convenient to deal with. This model, which we will call the *idealized model*, was introduced by Fountoulakis and Müller [11]. We will motivate it by looking in detail at the connection rule in the KPKVB model. For this we use Lemma 2.2.3, which tells us that $\vartheta(r_1, r_2)$ can be approximated by $2e^{\frac{R-r_1-r_2}{2}}$. Therefore, the approximate connection rule is

$$(r_1, \vartheta_1) \sim (r_2, \vartheta_2) \iff |\vartheta_1 - \vartheta_2|_{2\pi} \leq 2e^{\frac{R-r_1-r_2}{2}}.$$

We now change our coordinate system on $\mathcal{D}_R$ as follows. We scale the angle of a point by $\frac{1}{2}e^{R/2}$ and we replace the radial coordinate r by $R - r$. In other words, we replace (r, ϑ) by $(r', \vartheta') = (R - r, \frac{1}{2}e^{R/2}\vartheta)$. Note that

$$\begin{aligned}(r_1, \vartheta_1) \sim (r_2, \vartheta_2) &\iff |\vartheta_1 - \vartheta_2|_{2\pi} \leq 2e^{\frac{R-r_1-r_2}{2}} \\ &\iff \tfrac{1}{2}e^{R/2}|\vartheta_1 - \vartheta_2|_{2\pi} \leq e^{\frac{(R-r_1)+(R-r_2)}{2}},\end{aligned}$$

so the new approximate connection rule reads

$$(r_1', \vartheta_1') \sim (r_2', \vartheta_2') \iff |\vartheta_1' - \vartheta_2'|_{\pi e^{R/2}} \leq e^{\frac{r_1'+r_2'}{2}}.$$

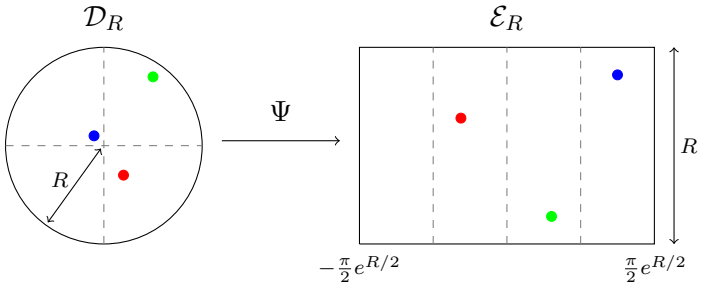

Figure 2.3: Ψ maps $\mathcal{D}_R$ to a rectangle $\mathcal{E}_R \subset \mathbb{R}^2$.

We will interpret the new coordinates as Euclidean x and y coordinates, with $R - r$ becoming the y coordinate and $\frac{1}{2}e^{R/2}\vartheta$ becoming the x coordinate. Put more formally, we define $\Psi : \mathcal{D}_R \to \mathbb{R}^2$ given by $\Psi : (r, \vartheta) \mapsto \left(\vartheta \cdot \frac{1}{2}e^{R/2}, R - r\right)$. The image of $\mathcal{D}_R$ under Ψ is the rectangle $\mathcal{E}_R = (-\frac{\pi}{2}e^{R/2}, \frac{\pi}{2}e^{R/2}] \times [0, R] \subset \mathbb{R}^2$ (Figure 2.3; we take the radial coordinates in $(-\pi, \pi]$). Using the map Ψ, we can map the random hyperbolic graph living on $\mathcal{D}_R$ to a graph living on $\mathcal{E}_R$. In light of the above derivations, we expect that the connection rule of the resulting graph will approximately be $(x, y) \sim (x', y') \iff |x - x'|_{\pi e^{R/2}} \leq e^{\frac{1}{2}(y+y')}$. The graph that we will use to approximate the

KPKVB random graph will be a graph Γ living on $\mathcal{E}_R$ that has this connection rule. We now need to determine an appropriate vertex set for Γ.

Let $X_1, X_2, \ldots \in \mathcal{D}_R$ be an infinite supply of points chosen independently according the (α, R)-distribution on $\mathcal{D}_R$. Let $G = G(N; \alpha, \nu)$ and $G_{\mathrm{Po}} = G_{\mathrm{Po}}(N; \alpha, \nu)$. Denote the number of vertices of G_{Po} by Z; then $Z \sim \mathrm{Po}(N)$. By taking $\{X_1, \ldots, X_N\}$ as the vertex set of G and $\{X_1, \ldots, X_Z\}$ as the vertex set of G_{Po}, we obtain a coupling between G and G_{Po}. Recall that $\{X_1, \ldots, X_Z\}$ can be viewed as the point set of a Poisson point process on $\mathcal{D}_R$. The Mapping Theorem for Poisson processes (Theorem 1.3.8) suggests that the vertex set of Γ could be given by a Poisson process on $\mathcal{E}_R$. The correct Poisson process turns out to have intensity function $f_{\alpha,\lambda}(x, y) = \mathbf{1}_{\mathcal{E}_R} \lambda e^{-\alpha y}$ for $\lambda = \frac{\nu\alpha}{\pi}$. We denote this Poisson process by $\mathcal{P}_\lambda$ and its point set by V_λ. The graph $\Gamma = \Gamma_\lambda$ that we will use has vertex set V_λ and as connection rule the rule $(x, y) \sim (x', y') \iff |x - x'|_{\pi e^{R/2}} \leq e^{\frac{1}{2}(y+y')}$described above.

Lemma 2.3.1 ([11], Lemma 26)**.** *Let $\alpha > \frac{1}{2}$. There exists a coupling such that a.a.s. $V_{\nu\alpha/\pi}$ is the image of the vertex set of G_{Po} under Ψ.*

Proof. The vertex set V of G_{Po} is the point set of a Poisson process on $\mathcal{D}_R$ with intensity function $f(r, \vartheta) = \frac{N}{2\pi} \frac{\alpha \sinh(\alpha r)}{\cosh(\alpha R) - 1}$. By Theorem 1.3.8, $\Psi(V)$ is a Poisson process on $\mathcal{E}_R$. By the changes of variables formula, we see that its intensity function $f_{\Psi(V)}$ satisfies

$$f_{\Psi(V)}(x, y) = \frac{f(\Psi^{-1}(x, y))}{|\det(J_\Psi)|},$$

where J_Ψ is the Jacobian of Ψ. We compute $|\det(J_\Psi)| = \begin{vmatrix} 0 & \frac{1}{2}e^{R/2} \\ -1 & 0 \end{vmatrix} = \frac{1}{2}e^{R/2}$ to find, writing $\lambda = \nu\alpha/\pi$,

$$f_{\Psi(V)}(x, y) = \frac{f(\Psi^{-1}(x, y))}{|\det(J_\Psi)|} = \frac{\nu e^{R/2}}{2\pi} \cdot \frac{\alpha \sinh(\alpha(R - y))}{\cosh(\alpha R) - 1} \cdot 2e^{-R/2} = \lambda e^{-\alpha y} \cdot \frac{1 - 2e^{2\alpha(y-R)}}{1 + e^{-2\alpha R} - 2e^{-\alpha R}}.$$

We now define independent Poisson processes $\mathcal{P}_0$, $\mathcal{P}_1$ and $\mathcal{P}_2$ on $\mathcal{E}_R$, with intensity functions respectively $f_{\min} = \min(f_{\alpha,\lambda}, f_{\Psi(V)})$, $f_1 = f_{\Psi(V)} - f_{\min}$ and $f_2 = f_{\alpha,\lambda} - f_{\min}$. Now $\mathcal{P}_0 \cup \mathcal{P}_1$ is a Poisson process with intensity function $f_{\Psi(V)}$ (Theorem 1.3.6) and $\mathcal{P}_0 \cup \mathcal{P}_2$ is a Poisson process with intensity function $f_{\alpha,\lambda}$. We define a coupling between $\Psi(V)$ and V_λ by setting $\Psi(V) = \mathcal{P}_0 \cup \mathcal{P}_1$ and $V_\lambda = \mathcal{P}_0 \cup \mathcal{P}_2$. It remains to show that this coupling has the required property that a.a.s. $\Psi(V) = V_\lambda$. This amounts to showing that $\mathcal{P}_1 \cup \mathcal{P}_2 = \emptyset$ holds a.a.s.. Note that by the above computation, $\mathcal{P}_1 \cup \mathcal{P}_2$ is a Poisson process with intensity

$$\begin{aligned} f_1(x, y) + f_2(x, y) &= \left| f_{\Psi(V)}(x, y) - f_{\alpha,\lambda}(x, y) \right| \\ &= \lambda e^{-\alpha y} \left| 1 - \frac{1 - e^{2\alpha(y-R)}}{1 + e^{-2\alpha R} - 2e^{-\alpha R}} \right| \\ &= \lambda e^{-\alpha y} \left| \frac{2e^{\alpha(y-R)} + o(1)}{1 + o(1)} \right| = O(e^{-\alpha y} e^{2\alpha(y-R)}) = O(e^{\alpha y - 2\alpha R}). \end{aligned}$$

We therefore have

$$\begin{aligned} \mathbb{E}|\mathcal{P}_1 \cup \mathcal{P}_2| &= \pi e^{R/2} \int_0^R O(e^{\alpha y - 2\alpha R}) \, \mathrm{d}y \\ &= O\left(e^{R/2} \int_0^R e^{\alpha y - 2\alpha R} \, \mathrm{d}y \right) = O(e^{R/2} e^{-\alpha R}) = O(e^{(\frac{1}{2} - \alpha)R}) = o(1), \end{aligned}$$

where we use the assumption $\alpha > \frac{1}{2}$ in the final step. □

Let $\tilde{X}_1, \tilde{X}_2, \ldots \in \mathcal{E}_R$ be the images of $X_1, X_2, \ldots$ under Ψ. On the coupling space of Lemma 2.3.1, a.a.s. we have $V_\lambda = \{\tilde{X}_1, \ldots, \tilde{X}_Z\}$ for the vertex set of Γ_λ. The following Lemma is similar to Lemma 29 in [11].

Lemma 2.3.2. *Let $\alpha > \frac{1}{2}$. On the coupling space of Lemma 2.3.1, a.a.s. it holds for $1 \le i, j \le Z$ that*

(i) if $r_i, r_j \ge \frac{1}{2}R$ and $\tilde{X}_i\tilde{X}_j \in E(\Gamma_{\nu\alpha/\pi})$, then $X_iX_j \in E(G_{\mathrm{Po}})$.

(ii) if $r_i + r_j \ge \frac{3}{2}R$, then $\tilde{X}_i\tilde{X}_j \in E(\Gamma_{\nu\alpha/\pi}) \iff X_iX_j \in E(G_{\mathrm{Po}})$.

Here r_i and r_j denote the radial coordinates of $X_i, X_j \in \mathcal{D}_R$.

Proof. We first deal with (i). Let A denote the number of pairs (i,j) with $i < j \le Z$ and $\min(r_i, r_j) \ge R/2$ such that $\tilde{X}_i$ and $\tilde{X}_j$ are neighbors in $\Gamma_{\nu\alpha/\pi}$, but X_i and X_j are not neighbors in G_{Po}. We write $\tilde{X}_i = (x_i, y_i)$ in cartesian coordinates and $X_i = (r_i, \vartheta_i)$ in hyperbolic polar coordinates. We have

$$A = \#\left\{i < j \le Z : \min(r_i, r_j) \ge R/2,\ |x_i - x_j|_{\pi e^{R/2}} \le e^{(y_i+y_j)/2} \quad \text{and} \quad |\vartheta_i - \vartheta_j|_{2\pi} > \vartheta(r_i, r_j)\right\}.$$

By Lemma 2.2.3, we know that $|\vartheta_i - \vartheta_j|_{2\pi} > \vartheta(r_i, r_j)$ implies

$$|x_i - x_j|_{\pi e^{R/2}} > \tfrac{1}{2}e^{R/2}\vartheta(r_i, r_j) \ge e^{(y_i+y_j)/2} - \frac{K}{2}\left(e^{-R+\frac{3}{2}\max(y_i,y_j)-\frac{1}{2}\min(y_i,y_j)}\right)$$

(the K is from Lemma 2.2.3), so $A \le \#\{i < j \le Z : A_{ij}\}$, where A_{ij} denotes the "bad" event

$$\{\min(r_i, r_j) \ge R/2\} \cap \left\{|x_i - x_j|_{\pi e^{R/2}} \in \left(e^{(y_i+y_j)/2} - \tfrac{K}{2}e^{-R+\frac{3}{2}\max(y_i,y_j)-\frac{1}{2}\min(y_i,y_j)}, e^{(y_i+y_j)/2}\right]\right\}.$$

Note that $p = \mathbb{P}(A_{ij})$ is independent of i and j, so we obtain

$$\mathbb{E}A \le \sum_{i,j} \mathbb{P}(i, j \le Z)\, p = p\,\mathbb{E}\tbinom{Z}{2} = \frac{pN^2}{2},$$

because $2\mathbb{E}\binom{Z}{2} = \mathbb{E}Z^2 - \mathbb{E}Z = \mathrm{Var}(Z) + (\mathbb{E}Z)^2 - \mathbb{E}Z = N + N^2 - N = N^2$. From the law of total expectation we have $p = \mathbb{E}[\mathbf{1}_{A_{ij}}] = \mathbb{E}[\mathbf{1}_{y_i,y_j \le R/2}\mathbb{E}[\mathbf{1}_{A_{ij}} \mid y_i, y_j]]$. If $y_i, y_j \le R/2$, the inner expectation equals

$$\mathbb{E}[\mathbf{1}_{A_{ij}} \mid y_i, y_j] = O\left(e^{-R+\frac{3}{2}\max(y_i,y_j)-\frac{1}{2}\min(y_i,y_j)}\right)(\tfrac{1}{2}\pi e^{R/2})^{-1} = O\left(e^{-\frac{3}{2}R+\frac{3}{2}\max(y_i,y_j)-\frac{1}{2}\min(y_i,y_j)}\right),$$

because the horizontal distance $|x_i - x_j|_{\pi e^{R/2}}$ follows a uniform distribution on $[0, \frac{1}{2}\pi e^{R/2}]$. Note that y_i, y_j are independent random variables with density function

$$f(y) = \frac{\mathbf{1}_{[0,R]}\lambda e^{-\alpha y}}{\int_0^R \lambda e^{-\alpha t}\,\mathrm{d}t} = \mathbf{1}_{[0,R]}\frac{\alpha\, e^{-\alpha y}}{1 - e^{-\alpha R}} = \mathbf{1}_{[0,R]}O(e^{-\alpha y}).$$

We find

$$\begin{aligned}
p &= \mathbb{E}\left[\mathbf{1}_{y_i,y_j \le R/2}O\left(e^{-\frac{3}{2}R+\frac{3}{2}\max(y_i,y_j)-\frac{1}{2}\min(y_i,y_j)}\right)\right] \\
&= O\left(\int_0^{R/2}\int_0^{R/2} e^{-\frac{3}{2}R+\frac{3}{2}\max(y_i,y_j)-\frac{1}{2}\min(y_i,y_j)}e^{-\alpha y_i}e^{-\alpha y_j}\,\mathrm{d}y_j\,\mathrm{d}y_i\right) \\
&= O\left(\int_0^{R/2}\int_{y_i}^{R/2} e^{-\frac{3}{2}R+\frac{3}{2}y_j-\frac{1}{2}y_i-\alpha y_i-\alpha y_j}\,\mathrm{d}y_j\,\mathrm{d}y_i\right) \\
&= O\left(e^{-\frac{3}{2}R}\int_0^{R/2} e^{(-\frac{1}{2}-\alpha)y_i}\int_{y_i}^{R/2} e^{(\frac{3}{2}-\alpha)y_j}\,\mathrm{d}y_j\,\mathrm{d}y_i\right) = O\left(e^{-\frac{3}{2}R}e^{\frac{1}{2}(\frac{3}{2}-\alpha)R}\right).
\end{aligned}$$

Using $\alpha > \frac{1}{2}$, it follows that

$$\mathbb{E}A \le \frac{pN^2}{2} = O(e^R)O\left(e^{-\frac{3}{2}R}e^{\frac{1}{2}(\frac{3}{2}-\alpha)R}\right) = O(e^{\frac{1}{4}(1-2\alpha)R}) = o(1),$$

so a.a.s. $A = 0$, as required. This completes the proof of (i).

The argument for (ii) is similar. Let B be the number of indices $i < j \le Z$ such that $\tilde{X}_i$ and $\tilde{X}_j$ are not neighbors in $\Gamma_{\nu\alpha/\pi}$ but X_i and X_j are neighbors in G_{Po} and such that furthermore $y_i + y_j \le R/2$. By Lemma 2.2.3 we have

$$B \le \#\left\{i < j \le Z : y_i + y_j \le R/2 \text{ and } |x_i - x_j|_{\pi e^{R/2}} \in (e^{(y_i+y_j)/2}, e^{(y_i+y_j)/2} + \tfrac{3}{2}e^{(3y_i+3y_j-2R)/2}]\right\}.$$

Let B_{ij} denote the "bad" event

$$\{y_i + y_j \le R/2\} \cap \left\{|x_i - x_j|_{\pi e^{R/2}} \in \left(e^{(y_i+y_j)/2}, e^{(y_i+y_j)/2} + \tfrac{3}{2}e^{(3y_i+3y_j-2R)/2}\right]\right\}.$$

As before, we have $\mathbb{E}B \le \frac{N^2 q}{2}$, where $q = \mathbb{P}(B_{ij})$. We have

$$q = \mathbb{E}[\mathbf{1}_{B_{ij}}] = \mathbb{E}[\mathbf{1}_{\{y_i+y_j\le R/2\}}\mathbb{E}[\mathbf{1}_{B_{ij}} \mid y_i, y_j]].$$

If $y_i + y_j \le R/2$, the inner expectation equals

$$\tfrac{3}{2}e^{(3y_i+3y_j-2R)/2}(\tfrac{1}{2}\pi e^{R/2})^{-1} = O(e^{\frac{3}{2}(y_i+y_j-R)}),$$

so we obtain

$$\begin{aligned}
\mathbb{E}B &= O\left(e^R\,\mathbb{E}\left[\mathbf{1}_{\{y_i+y_j\le R/2\}}e^{\frac{3}{2}(y_i+y_j-R)}\right]\right)\\
&= O\left(e^{-R/2}\int_0^{R/2}\int_0^{R/2}\mathbf{1}_{\{y_i+y_j\le R/2\}}e^{(\frac{3}{2}-\alpha)(y_i+y_j)}\,\mathrm{d}y_j\,\mathrm{d}y_i\right)\\
&= O\left(e^{-R/2}\int_0^{R/2}\int_0^{R/2}e^{(\frac{3}{2}-\alpha)R/2}\,\mathrm{d}y_j\,\mathrm{d}y_i\right) = O\left(R^2e^{(\frac{1}{2}-\alpha)R/2}\right) = o(1),
\end{aligned}$$

because $\alpha > \frac{1}{2}$. Hence a.a.s. there are no indices i, j such that $y_i + y_j \le R/2$, X_i and X_j are neighbors in G_{Po}, but $\tilde{X}_i$ and $\tilde{X}_j$ are not neighbors in $\Gamma_{\nu\alpha/\pi}$. Together with (i) this proves (ii). □

An example of G_{Po} and $\Gamma_{\nu\alpha/\pi}$ is shown in Figure 2.4.

Finally, we show that Lemma 2.3.1 and 2.3.2 remain true when conditioned on $Z = N$.

Lemma 2.3.3 (Lemma 2.3.1 conditional on $Z = N$)**.** *Let $\alpha > \frac{1}{2}$. On the coupling space of Lemma 2.3.1, conditional on $Z = N$, a.a.s. $V_{\nu\alpha/\pi}$ is the image of the vertex set of G_{Po} under Ψ. (We say that an event A happens a.a.s. conditional on B if $\mathbb{P}(A \mid B) \to 1$ as $N \to \infty$.)*

Proof. Write $V = \{X_1, \dots, X_Z\}$ and $\tilde{V} = V_{\nu\alpha/\pi}$. As in the proof of Lemma 2.3.1, there are independent Poisson processes $\mathcal{P}_0$, $\mathcal{P}_1$, $\mathcal{P}_2$ on $\mathcal{E}_R$ such that $\Psi(V) = \mathcal{P}_0 \cup \mathcal{P}_1$, $\tilde{V} = \mathcal{P}_0 \cup \mathcal{P}_2$ and $\mathbb{E}|\mathcal{P}_1|$, $\mathbb{E}|\mathcal{P}_2| = o(1)$. We now find

$$\begin{aligned}
\mathbb{P}(\tilde{V} = \Psi(V) \mid Z = N) &= \mathbb{P}(|\mathcal{P}_1| = |\mathcal{P}_2| = 0 \mid |\mathcal{P}_0| + |\mathcal{P}_1| = N)\\
&= \mathbb{P}(|\mathcal{P}_1| = 0 \mid |\mathcal{P}_0| + |\mathcal{P}_1| = N)\mathbb{P}(|\mathcal{P}_2| = 0),
\end{aligned}$$

because $\mathcal{P}_0$, $\mathcal{P}_1$ and $\mathcal{P}_2$ are independent. From $\mathbb{E}|\mathcal{P}_2| = o(1)$ it follows that $\mathbb{P}(|\mathcal{P}_2| = 0) = 1 - o(1)$. Furthermore, since the conditional distribution of a Poisson distributed variable given its sum with an independent Poisson distributed variable is binomial, we have $\mathbb{P}(|\mathcal{P}_1| = 0 \mid |\mathcal{P}_0| + |\mathcal{P}_1| = N) = \binom{N}{N}(1 - \mathbb{E}|\mathcal{P}_1|/N)^N = (1 - o(1)/N)^N = e^{-o(1)} = 1 - o(1)$, from which it follows that $\mathbb{P}(\tilde{V} = \Psi(V) \mid Z = N) = 1 - o(1)$. □

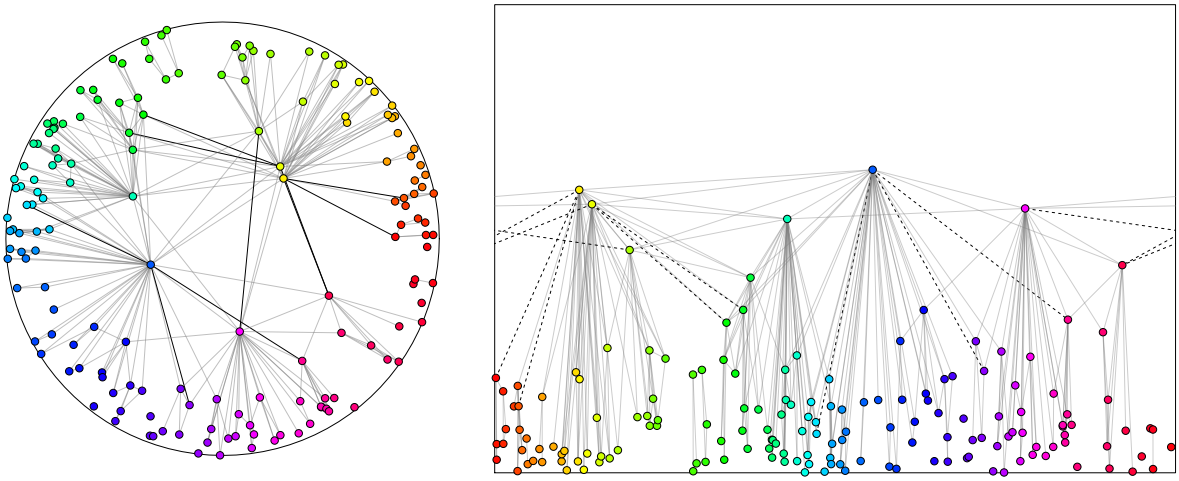

Figure 2.4: An example of the hyperbolic random graph G_{Po} (left) and the graph $\Gamma_{\nu\alpha/\pi}$ (right), under the coupling of Lemma 2.3.1. The graph G_{Po} is drawn in the native model of the hyperbolic plane, where a point with hyperbolic polar coordinates (r, ϑ) is plotted with Euclidean polar coordinates (r, ϑ). Points are colored based on their angular coordinate. The edges for which the coupling fails are drawn in black in the picture of G_{Po} and as dotted lines in the picture of $\Gamma_{\nu\alpha/\pi}$. The parameters used are $N = 200$, $\alpha = 0.8$ and $\nu = 1.3$.

Lemma 2.3.4 (Lemma 2.3.2 conditional on $Z = N$)**.** *Let $\alpha > \frac{1}{2}$. On the coupling space of Lemma 2.3.3, conditional on $Z = N$, a.a.s. it holds for $1 \leq i, j \leq Z$ that*

(i) if $r_i, r_j \geq \frac{1}{2}R$ and $\tilde{X}_i\tilde{X}_j \in E(\Gamma_{\nu\alpha/\pi})$, then $X_iX_j \in E(G_{\mathrm{Po}})$.

(ii) if $r_i + r_j \geq \frac{3}{2}R$, then $\tilde{X}_i\tilde{X}_j \in E(\Gamma_{\nu\alpha/\pi}) \iff X_iX_j \in E(G_{\mathrm{Po}})$.

Here r_i and r_j denote the radial coordinates of $X_i, X_j \in \mathcal{D}_R$.

Proof. Let A_Z denote the event that (i) or (ii) fails for some $i, j \leq Z$ and let A_N denote the event that (i) or (ii) fails for some $i, j \leq \min(N, Z)$. Note that $\mathbb{P}(A_Z \to 0$ by Lemma 2.3.2 and $\mathbb{P}(Z \geq N) \to \frac{1}{2}$ by (for example) the Central Limit Theorem. We now compute

$$\mathbb{P}(A_N \mid Z \geq N) \leq \frac{\mathbb{P}(A_N)}{\mathbb{P}(Z \geq N)} \leq \frac{\mathbb{P}(A_Z)}{\mathbb{P}(Z \geq N)} \overset{N\to\infty}{\longrightarrow} \frac{0}{1/2} = 0.$$

It follows that $\mathbb{P}(A_Z \mid Z = N) = \mathbb{P}(A_N \mid Z = N) = \mathbb{P}(A_N \mid Z \geq N) = o(1)$ so, conditioned on $Z = N$, a.a.s. (i) and (ii) hold. □

3

The diameter in the KPKVB model

In this chapter we study the diameter in the KPKVB model. In Section 3.1 we show that for $\alpha > \frac{1}{2}$, a.a.s. there are components of diameter $\Omega(\log N)$ [12, 19]. In Section 3.2 we show that for $\alpha \in (\frac{1}{2}, 1)$, a.a.s. every component has diameter $O(\log N)$. We show the same upper bound for the case $\alpha = 1$ and ν sufficiently large.

Together these results imply that the maximum diameter (over all components) in the KPKVB model is logarithmic in the number of vertices. This is also the case for the Chung–Lu model for complex networks [7]. In preferential attachment models, the diameter may even be of the order $\log \log N$ [9].

3.1 Logarithmic lower bound

In this section we prove an asymptotic lower bound for the diameter that holds asymptotically almost surely. The idea of the proof is from [19]. The result is that a.a.s. $G = G(N; \alpha, \nu)$ has a component of diameter $\Omega(\log N)$. Friedrich and Krohmer [12] elaborated on these results by showing that this lower bound in fact holds for the giant component. The general strategy of the proof is to find an induced path of logarithmic length close to the boundary of the disk. This path is found by independently exploring a number of disjoint sectors for such a path.

Theorem 3.1.1 (Asymptotic lower bound for the diameter)**.** *Let $\alpha > \frac{1}{2}$. A.a.s., G has a component with diameter $\Omega(\log N)$.*

Proof. We define G^δ to be the graph resulting from G after removal of all vertices in $B_0(\varepsilon R)$, where $\varepsilon = \frac{1}{2}(1 - \frac{1}{2\alpha})$. By Lemma 2.2.2 we know that a.a.s. $G = G^\delta$. We define G^δ_{Po} analogously. We start by studying G_{Po}. Below we frequently make use of the fact that the number of vertices of G_{Po} in disjoint subregions of $\mathcal{D}_R$ is independent.

We divide $\mathcal{D}_R$ into sectors S_0, S_1, S_2, ... of angle $\frac{1}{2}e^{-R/2} = \Theta(N^{-1})$. Consider a sector S_i. Let A_i be the subset of S_i consisting of points at distance at least $R - 1$ from the origin (i.e. at distance at most 1 from the boundary of the disk). We define the following events:

- $E_i = \{A_i$ contains exactly one vertex v_i of $G_{\mathrm{Po}}\}$;
- $F_i = \{E_i$ happens and v_i has no neighbors in G^δ_{Po} that lie in $B_0(R-1)\}$.

We claim that F_i happens with probability $e^{-\Theta(1)}$. The number of vertices of G_{Po} in A_i follows a Poisson distribution with mean

$$N\mu(A_i) = \Theta(e^{R/2})\Theta(e^{-R/2}) \int_{R-1}^{R} \Theta(e^{(r-R)\alpha})\,\mathrm{d}r = \Theta(1),$$

because $f(r, \vartheta) = \Theta(e^{(r-R)\alpha})$ (see the proof of Lemma 2.2.4). It follows that

$$\mathbb{P}(E_i) = N\mu(A_i)e^{-N\mu(A_i)} = \Theta(1)e^{-\Theta(1)} = e^{-\Theta(1)}.$$

We have $\mathbb{P}(F_i) = \mathbb{P}(F_i \mid E_i)\mathbb{P}(E_i)$, so we now consider $\mathbb{P}(F_i \mid E_i)$. Note that a vertex u in A_i is isolated with probability $e^{-N\mu(B_0(R)\cap B_u(R))} = e^{-\Theta(e^{R/2})\Theta(e^{R/2})} = e^{-\Theta(1)}$ by Lemma 2.2.4. We find

$$\mathbb{P}(F_i \mid E_i) \leq \mathbb{P}(v_i \text{ is isolated in } G_{\mathrm{Po}} \mid E_i) = e^{-\Theta(1)},$$

so we indeed have $\mathbb{P}(F_i) = e^{-\Theta(1)}$. Now consider consecutive sectors S_1, S_2, ..., S_p. Suppose the event $\bigcap_{i=1}^p E_i$ happens. The event F_i prescribes that there are no vertices of G_{Po}^δ that lie in $B_0(R-1) \cap B_{v_i}(R)$. We call this region B_i. We also choose subregions $B_i' \subset B_i$ for each i, such that B_1', ..., B_p' form a partition of $\bigcup_{i=1}^p B_i$. Let $G_i \supset F_i$ denote the event that B_i' contains no vertices of G_{Po}^δ. Note that the events G_1, ..., G_p, E_1, ..., E_p are all independent because they concern disjoint subregions of $\mathcal{D}_R$. We find

$$\begin{aligned}\mathbb{P}\left(\bigcap_{i=1}^p F_i \,\middle|\, \bigcap_{i=1}^p E_i\right) &= \mathbb{P}\left(\left(\bigcup_{i=1}^p B_i\right) \text{ contains no vertices of } G_{\text{Po}}^\delta \,\middle|\, \bigcap_{i=1}^p E_i\right) = \mathbb{P}\left(\bigcap_{i=1}^p G_i \,\middle|\, \bigcap_{i=1}^p E_i\right) \\ &= \prod_{i=1}^p \mathbb{P}\left(G_i \,\middle|\, \bigcap_{i=1}^p E_i\right) \geq \prod_{i=1}^p \mathbb{P}\left(F_i \,\middle|\, \bigcap_{i=1}^p E_i\right) = \prod_{i=1}^p (F_i \mid E_i) = e^{-p\Theta(1)}.\end{aligned}$$

It follows that

$$\mathbb{P}\left(\bigcap_{i=1}^p F_i\right) = \mathbb{P}\left(\bigcap_{i=1}^p F_i \,\middle|\, \bigcap_{i=1}^p E_i\right) \prod_{i=1}^p \mathbb{P}\left(E_i\right) = e^{-p\Theta(1)} e^{-p\Theta(1)} = e^{-p\Theta(1)}.$$

We now consider what we know if $F = \bigcap_{i=1}^p F_i$ happens. By definition then A_1, ..., A_p each contain a vertex $v_i \in A_i$ that have no neighbors in $B_0(R-1)$. The angular distance between v_i and v_{i+1} is at most $e^{-R/2} \leq 2e^{-R/2} - O(e^{-R})$ and it follows from Lemma 2.2.3 that v_i and v_{i+1} are neighbors in G_{Po}. In particular, v_1 and v_p lie in the same component of G_{Po}. A path from v_1 to v_p in G_{Po}^δ lies completely inside $\mathcal{D}_R \setminus B_0(R-1)$. The angular distance between v_1 and v_p is at least $\Theta(pe^{R/2})$. Each step, the path travels an angular distance of at most

$$2e^{(R-(R-1)-(R-1))/2} + O(e^{R-(R-1)-(R-1)}) \leq 6e^{-R/2}$$

for sufficiently large R (we again use Lemma 2.2.3). It follows that the path takes at least $\Theta(p)$ steps, so G_{Po}^δ has diameter at least $\Omega(p)$ if $\bigcap_{i=1}^p F_i$ happens.

We now take $p = cR = \Theta(\log N)$ for a choice of c to be specified later. A neighbor of a vertex in A_i that lies outside $B_0(\varepsilon R)$ lies at angular distance at most $\Theta(e^{(R-\varepsilon R-(R-1))/2}) = \Theta(e^{-\varepsilon R/2})$ from A_i. It follows that to determine whether the event F happens, we need to explore a big sector of total angle $\Theta(e^{-\varepsilon R/2}) + p \cdot \frac{1}{2} e^{-R/2} + \Theta(e^{-\varepsilon R/2}) = \Theta(e^{-\varepsilon R/2})$ (recall that $p = O(R)$). This means that we can make $\Theta(e^{\varepsilon R/2})$ big sectors, in each of which we can run an independent trial of the event F. The probability that all of them fail is at most

$$\begin{aligned}(1 - e^{-p\Theta(1)})^{\Theta(e^{\varepsilon R/2})} &\leq \exp\left(-e^{-p\Theta(1)}\Theta(e^{\varepsilon R/2})\right) \\ &= \exp\left(-\Theta\left(e^{\varepsilon R/2 - \Theta(1)cR}\right)\right) \leq \exp(-R/2) = O(N^{-1})\end{aligned}$$

where the last inequality holds for sufficiently small c. It follows that for c small enough, with probability $1 - O(N^{-1})$ there is at least one sector where the event F happens. Therefore, with probability $1 - O(N^{-1})$ there is a component of G_{Po}^δ with diameter $\Theta(cR) = \Omega(\log N)$.

It follows from Lemma 2.1.1 that a.a.s. the graph G^δ also has a component of diameter $\Omega(\log N)$. If we combine this result with Lemma 2.2.2, we see that a.a.s. G has a component with diameter $\Omega(\log N)$. □

3.2 Logarithmic upper bound

In this section we prove an asymptotic upper bound for the diameter. The main result is the following.

Theorem 3.2.1 (Asymptotic upper bound for the diameter)**.** *Let $\alpha, \nu > 0$. Then the following holds:*

(i) For $\frac{1}{2} < \alpha < 1$ and ν arbitrary, a.a.s. every component of $G(N; \alpha, \nu)$ has diameter $O(\log(N))$.

(ii) For $\alpha = 1$ and ν sufficiently large, a.a.s. every component of $G(N; \alpha, \nu)$ has diameter $O(\log(N))$.

By the triangle inequality, all vertices of $G = G(N; \alpha, \nu)$ inside $B_0(R/2)$ (i.e. the vertices at distance at most $R/2$ from the origin) form a clique. Let G^Δ be the subgraph of G induced by the vertices outside this clique. We define G^Δ_{Po} similarly. (Note that in comparison with the graphs G^δ and G^δ_{Po} from Section 3.1, we remove more vertices.) By adding back the vertices in $B_0(R/2)$, the diameter cannot grow too much:

Lemma 3.2.2. *If every component of G^Δ has diameter at most d, then every component of G has diameter at most $2d+3$. Similarly, if every component of G^Δ_{Po} has diameter at most d, then every component of G_{Po} has diameter at most $2d+3$.*

Proof. Let C be a component of G. If C contains no vertices inside $B_0(R/2)$, then C is a component of G^Δ as well. We then immediately find that C has diameter at most d. If not, then there is a path of length at most $d+1$ from any vertex in C to a vertex in $B_0(R/2)$. Because the vertices in $B_0(R/2)$ form a clique, we then find that C has diameter at most $(d+1)+1+(d+1) = 2d+3$, as required. The proof for G_{Po} is identical. □

In light of Lemma 3.2.2, it suffices to prove bounds for the diameter for the graphs G^Δ and G^Δ_{Po}. In our proofs, we will make use of the idealized model, which was introduced earlier.

Recall from Section 2.3 that Γ_λ is a graph with vertex set V_λ, where two vertices (x, y) and (x', y') are connected by an edge if and only if $|x - x'|_{\pi e^{R/2}} \leq e^{\frac{1}{2}(y+y')}$. Here V_λ is the point set of the Poisson process $\mathcal{P}_\lambda$ on $\mathcal{E}_R = (-\frac{\pi}{2}e^{R/2}, \frac{\pi}{2}e^{R/2}] \times [0, R] \subset \mathbb{R}^2$ with intensity $\mathbf{1}_{\mathcal{E}_R}\lambda e^{-\alpha y}$. Analogously to the definitions above, we also define the subgraph Γ^Δ_λ of Γ_λ, induced by the vertices in $V^\Delta_\lambda = \{(x, y) \in V_\lambda : y \leq R/2\}$. This graph lives on the lower half $(-\frac{\pi}{2}e^{R/2}, \frac{\pi}{2}e^{R/2}] \times [0, R/2]$ of $\mathcal{E}_R$.

From Lemma 2.3.1 and Lemma 2.3.2, we know that for $\lambda = \nu\alpha/\pi$, the graphs Γ_λ and G_{Po} are rather similar. The graphs Γ^Δ_λ and G^Δ_{Po} are even more similar: in fact, from Lemma 2.3.2 it follows that a.a.s. Γ^Δ_λ is isomorphic to a spanning subgraph of G^Δ_{Po}. We will therefore continue by studying the diameter of Γ_λ and Γ^Δ_λ.

Discretization of the model

We start in a somewhat more general setting, where $V \subset \mathcal{E}_R$ is any finite set of points and Γ is the graph with vertex set V and connection rule $(x, y) \sim (x', y') \iff |x - x'|_{\pi e^{R/2}} \leq e^{\frac{1}{2}(y+y')}$. We dissect $\mathcal{E}_R$ into a number of rectangles, which have the property that vertices of Γ in rectangles with nonempty intersection are necessarily connected by an edge. This is done as follows. First, divide $\mathcal{E}_R$ into $\ell + 1$ layers L_0, L_1, …, L_ℓ, where

$$L_i = \{(x, y) \in \mathcal{E}_R : i\log(2) \leq y < (i+1)\log(2)\}$$

for $i < \ell$ and $L_\ell = \{(x, y) \in \mathcal{E}_R : y \geq \ell\log(2)\}$. Here ℓ is defined by $\ell = \lfloor \frac{\log(6\pi)+R/2}{\log(2)} \rfloor$, such that $6\pi e^{R/2} \geq 2^\ell > 3\pi e^{R/2}$. We divide L_i into $2^{\ell-i}$ (closed) rectangles of equal width $2^{i-\ell} \cdot \pi e^{R/2} = 2^i \cdot b$, where $b = 2^{-\ell} \cdot \pi e^{R/2} \in [\frac{1}{6}, \frac{1}{3})$ is the width of a rectangle in the lowest layer L_0 (Figure 3.1). In each layer, one of the rectangles has its left edge on the line $x = 0$. We have now partitioned $\mathcal{E}_R$ into $2^{\ell+1} - 1 = O(N)$ boxes.

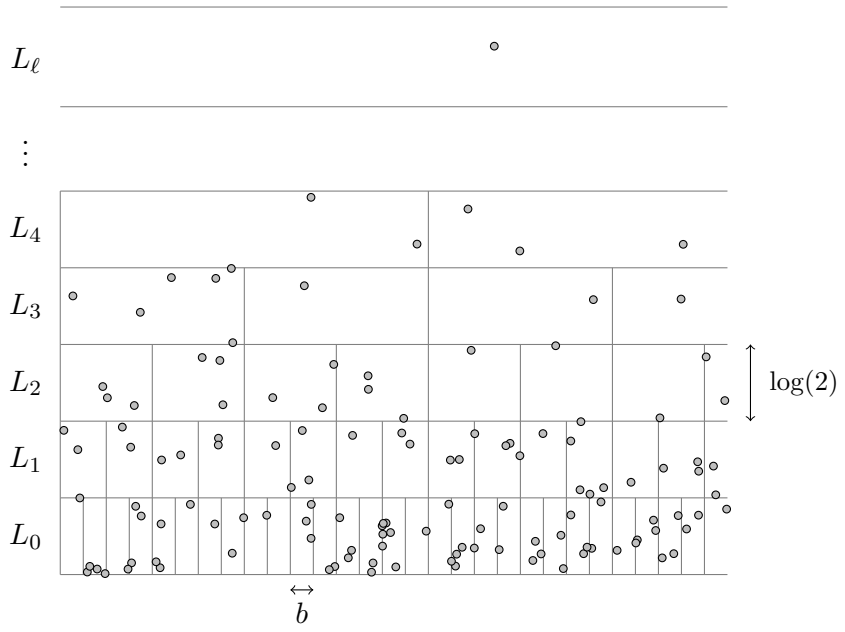

Figure 3.1: Left: Partioning $\mathcal{E}_R$ with boxes. All layers except L_ℓ have height log(2). The boxes in layer L_i have width $2^i b$, where $b \in [\frac{1}{6}, \frac{1}{3})$ is the width of a box in L_0. The small circles serve as an example of V.

The boxes are the vertices of a graph $\mathcal{B}$ in which two boxes are connected if they share at least a corner (Figure 3.2, left). Here we identify the left and right edge of $\mathcal{E}_R$ with each other, so that (for example) also the leftmost and rightmost box in each layer become neighbors. We will call a box *active* if it contains a vertex of Γ and *inactive* otherwise. The dissection has the following properties:

Lemma 3.2.3. *(i) If vertices of Γ lie in boxes that are neighbors in $\mathcal{B}$, then they are connected by an edge in Γ.*

(ii) The number of boxes that lie (partly) above the line $y = R/2$ is at most 63.

Proof. We start with (i). Consider two points (x, y) and (x', y') that lie in boxes that are neighbors in $\mathcal{B}$. Suppose that the lowest of these two points lies in L_i. Then $y, y' \geq i \log(2)$. Furthermore, the horizontal distance between (x, y) and (x', y') is at most 3 times the width of a box in L_i. It follows that

$$|x - x'|_{\pi e^{R/2}} \leq 3 \cdot 2^i \cdot b \leq 2^i \leq e^{\frac{1}{2}(y+y')},$$

so (x, y) and (x', y') are indeed connected in Γ.

To show (ii), we note that the first layer L_i that extends above the line $y = R/2$ has index $i = \lfloor \frac{R/2}{\log 2} \rfloor$. Therefore, we must count the boxes in the layers L_i, L_{i+1}, ..., L_ℓ, of which there are $2^{\ell-i+1} - 1$. We have

$$\ell - i + 1 = \left\lfloor \frac{\log(6\pi) + R/2}{\log 2} \right\rfloor - \left\lfloor \frac{R/2}{\log 2} \right\rfloor + 1 \leq \left\lceil \frac{\log(6\pi)}{\log 2} \right\rceil + 1 = 6,$$

so there are indeed at most $2^6 - 1 = 63$ boxes that extend above the line $y = R/2$. □

Let $\mathcal{B}^*$ be the subgraph of $\mathcal{B}$ where we remove the edges between boxes that have only a single point in common (Figure 3.2). Note that $\mathcal{B}^*$ is a planar graph and that $\mathcal{B}$ is obtained from $\mathcal{B}^*$

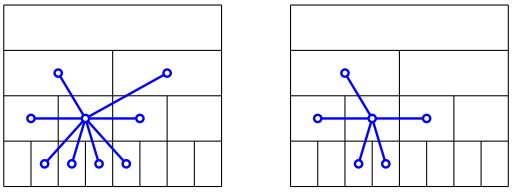

Figure 3.2: The connection rules of $\mathcal{B}$ and $\mathcal{B}^*$. Left: a box with its 8 neighbors in $\mathcal{B}$. Right: a box with its 5 neighbors in $\mathcal{B}^*$.

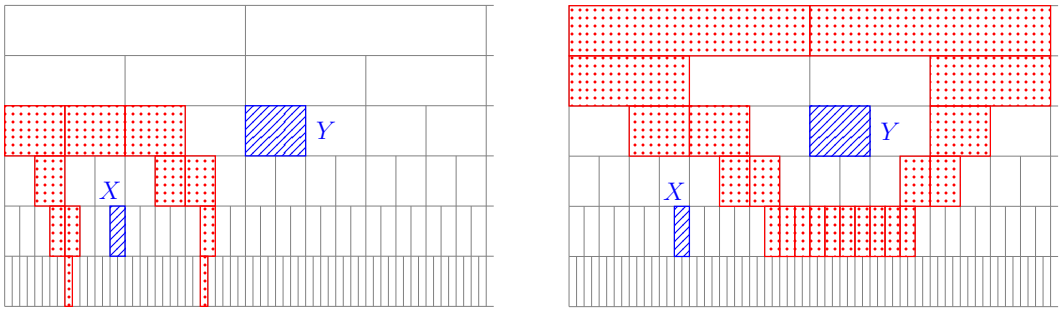

Figure 3.3: If two blue boxes X and Y are not connected by a path of blue (striped) boxes, then a red (dotted) walk exists that intersects every path in $\mathcal{B}$ from X from Y (Observation 3.2.4). This walk can be chosen such that it either connects two boxes in L_0 (left) or is cyclic (right).

by adding the diagonals of each face ([17] deals with a more general notation of *matching pairs* of graphs). We make the following observation (Figure 3.3; compare Proposition 2.1 in [17]) for later reference. The idea of the proof is from Bollobás ([6], p. 13 – 15).

Observation 3.2.4. *Suppose each box in $\mathcal{B}$ is colored red or blue. If there is no path of blue boxes in $\mathcal{B}$ between two blue boxes X and Y, then $\mathcal{B}^*$ (and hence also $\mathcal{B}$) contains a walk of red boxes Q that intersects every walk (and hence also every path) in $\mathcal{B}$ from X to Y.*

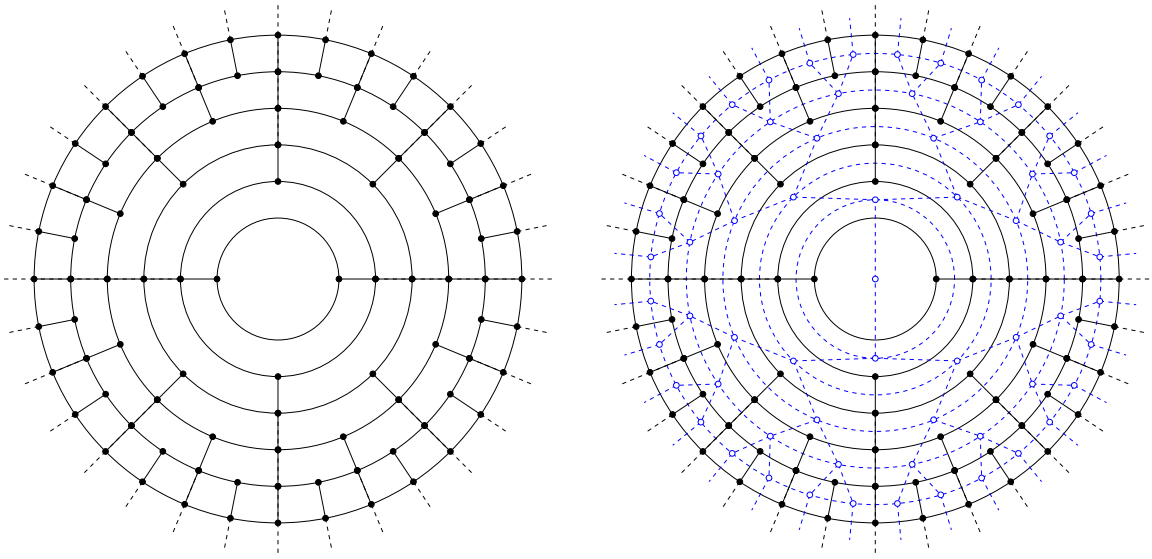

Figure 3.4: Left: the graph $\mathcal{D}$. Right: the graph $\mathcal{D}$ and its dual $\mathcal{D}^*$ (dashed).

Proof. We construct an infinite graph $\mathcal{D}$ as follows. The vertex set of $\mathcal{D}$ is the set of all points in the Euclidean plane whose polar coordinates (r, ϑ) have the property that r is a positive integer and ϑ is an integral multiple of $\pi/2^{r-1}$. This means that for each positive integer r there are 2^r vertices of $\mathcal{D}$ on the circle with radius r centered at the origin. We connect vertices by an edge if they are adjacent points on the same circle, or if they have the same angular coordinate and their radii are 1 apart (Figure 3.4, left). Clearly, $\mathcal{D}$ is a planar graph. Let $\mathcal{D}^*$ denote the dual of $\mathcal{D}$ (Figure 3.4, right).

There is a natural bijection between $\mathcal{B}$ and the vertices of $\mathcal{D}^*$ within the circle with radius $\ell+1$ centered at the origin, in which the layer L_i corresponds to the annulus $\{\vartheta \in [\ell-i, \ell-i+1]\}$. Two vertices are connected in $\mathcal{D}^*$ if and only if the corresponding boxes in $\mathcal{B}$ share at least an edge, so these vertices of $\mathcal{D}^*$ form a subgraph $\mathcal{D}^*_\ell$ of $\mathcal{D}^*$ isomorphic to $\mathcal{B}^*$.

If each box in $\mathcal{B}$ is colored red or blue then we also obtain a coloring of $\mathcal{D}^*$ as follows: the vertices in $\mathcal{D}^*_\ell$ that correspond to a blue box in $\mathcal{B}$ are colored blue, and all other vertices in $\mathcal{D}^*$ are colored red. We color the edges of $\mathcal{D}$ that are adjacent to at least one blue face (i.e. a blue vertex of $\mathcal{D}^*$) blue and all other edges red.

Now consider blue boxes X and Y such that $\mathcal{B}$ does not contain a path of blue boxes from X and Y. The box X corresponds to some blue vertex in $\mathcal{D}^*_\ell$, i.e. a blue face of $\mathcal{D}$. We choose one vertex x adjacent to this face and we let C_x denote the set of vertices of $\mathcal{D}$ that can be reached from x by a path of blue edges. We define y and C_y similarly. Because $\mathcal{B}$ does not contain a path of blue boxes from X to Y, $\mathcal{D}$ does not contain a path of blue edges from x to y. We therefore must have $C_x \cap C_y = \emptyset$. The graph $\mathcal{D} \setminus C_x$, obtained by removing the vertices in C_x, has a unique infinite component C_x^∞. Let ∂C_x denote the set of edges of $\mathcal{D}$ that connect a vertex in C_x with a vertex in C_x^∞. We orient each edge in ∂C_x towards the vertex in C_x^∞. For each edge $\overrightarrow{ab} \in \partial C_x$ with $a \in C_x$ and $b \in C_x^\infty$, we can consider the dual edge $\overrightarrow{uv}$, oriented such that a is to the right of this edge. This edge connects two red faces u and v (the edge $\overrightarrow{ab}$ is red because $b \notin C_x$, so both faces adjacent to this edge are red). Let $(\partial C_x)^*$ denote the set of these dual edges.

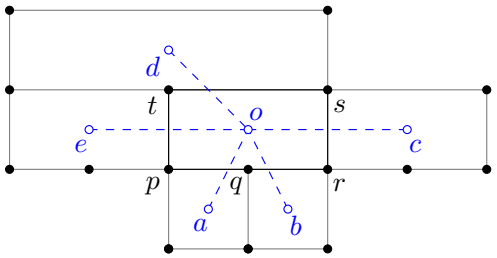

Figure 3.5: Every edge in $(\partial C_x)^*$ has a successor.

We claim that for each such dual edge $\overrightarrow{uv} \in (\partial C_x)^*$ there is a successor $\overrightarrow{vw} \in (\partial C_x)^*$. Consider an edge of $(\partial C_x)^*$ that points to the face o (Figure 3.5). The case that o is the face containing the origin is straightforward, so we suppose this is not the case. Then there are 5 vertices of $\mathcal{D}$ adjacent to o, which we call p, q, r, s, t (Figure 3.5).

The edge of $(\partial C_x)^*$ with head o has tail a, b, c, d or e as in Figure 3.5. If the edge is $\overrightarrow{ab}$, then we have $q \in C_x$ and $p \notin C_x$. If $t \in C_x$ we have $\overrightarrow{oe} \in (\partial C_x)^*$. If $t \notin C_x$ but $s \in C_x$ we have $\overrightarrow{od} \in (\partial C_x)^*$. If $s, t \notin C_x$ but $r \in C_x$ we have $\overrightarrow{oc} \in (\partial C_x)^*$. If finally $r, s, t \notin C_x$ we have $\overrightarrow{ob} \in (\partial C_x)^*$. We conclude that the edge $\overrightarrow{ab}$ has a successor in $(\partial C_x)^*$. The arguments for the edges $\overrightarrow{bo}$, $\overrightarrow{co}$, $\overrightarrow{do}$ and $\overrightarrow{eo}$ are completely similar.

Because $(\partial C_x)^*$ is a finite directed graph in which each edge has a successor, we find that $(\partial C_x)^*$ contains a cycle Q_x. We draw Q_x in the plane by connecting the centers of the relevant faces as in Figure 3.4, right. Note that Q_x separates the plane into two components by the Jordan

Curve Theorem. Furthermore, C_x^∞ must lie completely outside Q_x because Q_x only crosses edges of $\mathcal{D}$ in ∂C_x and C_x^∞ is infinite. It follows that C_x lies inside Q_x.

Since $C_x \cap C_y = \emptyset$, C_y lies either completely inside Q_x or completely outside Q_x. In the first case, it is easy to see that x lies outside Q_y. In the second case, y lies outside Q_x. Without loss of generality, we assume that y lies outside Q_x. The faces in Q_x form a cycle in $\mathcal{D}^*$. Each path in $\mathcal{D}^*$ from X to Y contains at least one face of this cycle, because a corresponding path in $\mathcal{D}$ from x to y crosses Q_x. The intersection of Q_x and $\mathcal{D}_\ell^*$ is either all of Q_x (in which case the corresponding boxes form a red cycle Q in $\mathcal{B}^*$ with the required property) or a union of paths, starting and ending in a face that corresponds to a box in L_0. Each of these paths borders a component of $\mathcal{D}_\ell^* \cap C_x^\infty$. The path bordering the component containing y corresponds to a path of boxes Q in $\mathcal{B}^*$ starting and ending in L_0. This path has the required property, because removing it separates $\mathcal{D}_\ell^*$ into two components, with one containing x and the other containing y.

We have now in all cases found the required walk Q of red boxes in $\mathcal{B}^*$ with the property that each path in $\mathcal{B}$ from X to Y contains at least one box in Q. □

Constructing short paths

We will use the boxes defined in the previous section to construct short paths between vertices of Γ. Recall that $V \subset \mathcal{E}_R$ is a finite set of points and Γ is the graph with vertex set V and connection rule $(x, y) \sim (x', y') \iff |x - x'|_{\pi e^{R/2}} \leq e^{\frac{1}{2}(y+y')}$.

One can easily deduce that the graph Γ has the following geometric properties:

Lemma 3.2.5 ([11], Lemma 3)**.** *Let x, y, z, $w \in V$.*

(i) If $xy \in E(\Gamma)$ and z lies above the line segment $[x, y]$ (i.e. $[x, y]$ intersects the segment joining z and the projection of z on the horizontal axis), then at least one of xz and yz is also present in Γ.

(ii) If xy, $wz \in E(\Gamma)$ and the segments $[x, y]$ and $[z, w]$ intersect, then at least one of the edges xw, xz, yw and yz is also present in Γ. In particular, $\{x, y, z, w\}$ is a connected subset of Γ.

Proof. Write $x = (x_0, x_1)$, $y = (y_0, y_1)$, $z = (z_0, z_1)$ and $w = (w_0, w_1)$.

For (i) we assume without loss of generality that $x_1 = \min(x_1, y_1)$. It follows that $z_1 \geq x_1$, because z lies above $[x, y]$. We now find

$$|z_0 - y_0|_{\pi e^{R/2}} \leq |x_0 - y_0|_{\pi e^{R/2}} \leq e^{\frac{1}{2}(x_1+y_1)} \leq e^{\frac{1}{2}(z_1+y_1)},$$

so yz is present in Γ.

For (ii) we assume without loss of generality that $x_0 \leq w_0 \leq y_0 \leq z_0$. Still without loss of generality, we can also assume that $w_1 \leq y_1$. From

$$|y_0 - z_0|_{\pi e^{R/2}} \leq |w_0 - z_0|_{\pi e^{R/2}} \leq e^{\frac{1}{2}(w_1+z_1)} \leq e^{\frac{1}{2}(y_1+z_1)}$$

we now conclude that the edge yz is present in Γ. □

We now prove a lemma that allows us to compare paths in Γ with walks in $\mathcal{B}$. This will enable us to translate information about Γ (such as that two boxes contain vertices in the same component of Γ) to information about the states of the boxes.

Lemma 3.2.6. *Suppose boxes $X, Y \in \mathcal{B}$ contain vertices $x, y \in V$ respectively that lie in the same component of Γ. Then $\mathcal{B}$ contains a walk $X = B_0, B_1, \ldots, B_n = Y$ with the following property:*

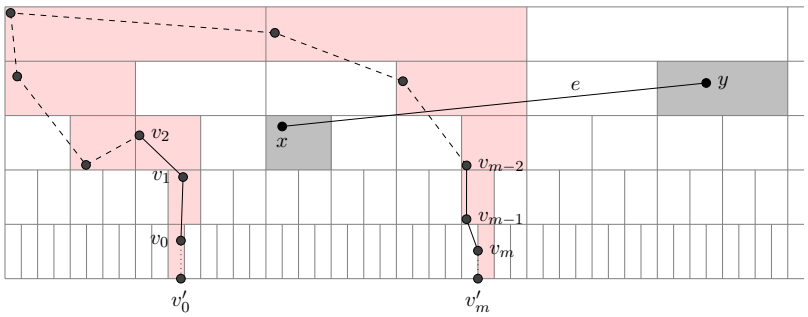

Figure 3.6: Proof of Lemma 3.2.6. The edge e of Γ connects vertices x and y. If a red walk of boxes exists that separates the boxes containing x and y, then e intersects one of the segments $[v_i, v_{i+1}]$, $[v_0, v'_0]$ or $[v_m, v'_m]$. This contradicts the assumption that no red box contains a neighbor of x or y.

(∗) *if B_i and B_j are active but B_{i+1}, B_{i+2}, …, B_{j-1} are not, then Γ has vertices $a \in B_i$, $b \in B_j$ that are connected in Γ by a path of length at most* 3.

Proof. We prove the statement by induction on the length of the shortest path from x to y in Γ.

First suppose that this length is 1, so that there is an edge e connecting x and y. We claim that a walk $X = B_0, B_1, \ldots, B_n = Y$ in $\mathcal{B}$ exists with the property that if B_i is active, then B_i contains a neighbor of x or y. For this we use Lemma 3.2.4. We color a box blue if it is either inactive or active and contains a neighbor of x or y. All other boxes are colored red. Note that X and Y are blue, because X contains the neighbor x of y and Y contains the neighbor y of x. We intend to show that $\mathcal{B}$ contains a blue path from X to Y. Aiming for a contradiction, we suppose that this is not the case. By Lemma 3.2.4, there must then exist a red walk $S = S_0, S_1, \ldots, S_m$ that intersects each path in $\mathcal{B}$ from X to Y. If we remove S from $\mathcal{E}_R$ then $\mathcal{E}_R \backslash S$ falls apart in a number of components. Because there is no path in $\mathcal{B}$ from X to Y that does not intersect S, X and Y lie in different components. We therefore say that S *separates* X and Y. We let s_i denote the center of S_i and we also choose vertices $v_i \in V \cap S_i$ for all i (these vertices exist because all red boxes are active; see Figure 3.6). By Lemma 3.2.3(i), v_i and v_{i+1} are neighbors in Γ for each i.

We may assume that either S_0 and S_m are both boxes in the lowest layer L_0, or S_0 and S_m are adjacent in $\mathcal{B}$ (Figure 3.3). In the latter case, we consider the polygonal line S' consisting of the line segments $[s_0, s_1]$, $[s_1, s_2]$, …, $[s_m, s_0]$, each of which lies completely inside boxes in S. Because S separates X and Y, S' separates x and y. If we replace each s_i by the corresponding vertex v_i, S' is replaced by the polygonal line through the points $v_0, v_1, \ldots, v_m$. This polygonal line consists of edges of Γ. Each of these edges passes through boxes in S and maybe also boxes adjacent to boxes in S. In particular, none of these edges can pass through X, because X is not adjacent to a box in S (this box should then have been blue by Lemma 3.2.3(i)). From this it follows that the polygonal line through the points $v_0, v_1, \ldots, v_m$ also separates x and y. Therefore, the edge e crosses an edge $[v_i, v_{i+1}]$ of Γ (Figure 3.6). By Lemma 3.2.5(ii) this means that v_i or v_{i+1} neighbors x or y, which is a contradiction because v_i and v_{i+1} do not lie in a blue box.

We are left with the case that S_0 and S_m lie in the lowest layer L_0. Let v'_0 and v'_m denote the projections of v_0 and v_m, respectively, on the horizontal axis. By an analogous argument, we find that the polygonal line through $v'_0, v_0, v_1, \ldots, v_m, v'_m$ separates x and y. We now see that e either crosses an edge $[v_i, v_{i+1}]$ (we then find a contradiction with Lemma 3.2.5(ii)) or one of the segments $[v_0, v'_0]$ and $[v_m, v'_m]$ (we then find a contradiction with Lemma 3.2.5(i)). From the contradiction we conclude that a blue path must exist connecting X and Y.

We have now shown that if x and y are neighbors in Γ, there exists a walk $X = B_0, B_1, \ldots, B_n = Y$ such that the B_i that are active contain a neighbor of x or y. This means that if B_i, B_{i+1},

$\ldots$, B_j are such that B_i and B_j are active but B_{i+1}, $\ldots$, B_{j-1} are not, then B_i contains a vertex a that neighbors x or y and B_j contains a vertex b that neighbors x or y. Now $d_\Gamma(a,b) \leq 3$ follows from the fact that both a and b neighbor an endpoint of the same edge e.

We conclude that if x and y are neighbors in Γ, then a walk satisfying $(*)$ exists. Now suppose that the statement holds whenever x and y satisfy $d_\Gamma(x,y) \leq k$ and consider two vertices x and y with $d_\Gamma(x,y) = k+1$. Choose a neighbor y' of y such that $d_\Gamma(x,y') = k$. Let Y' be the active box containing y'. By the induction hypothesis, there exists walks from X to Y' and from Y' to Y satisfying $(*)$. By concatenating these two walks we obtain a walk from X to Y satisfying $(*)$, as desired. □

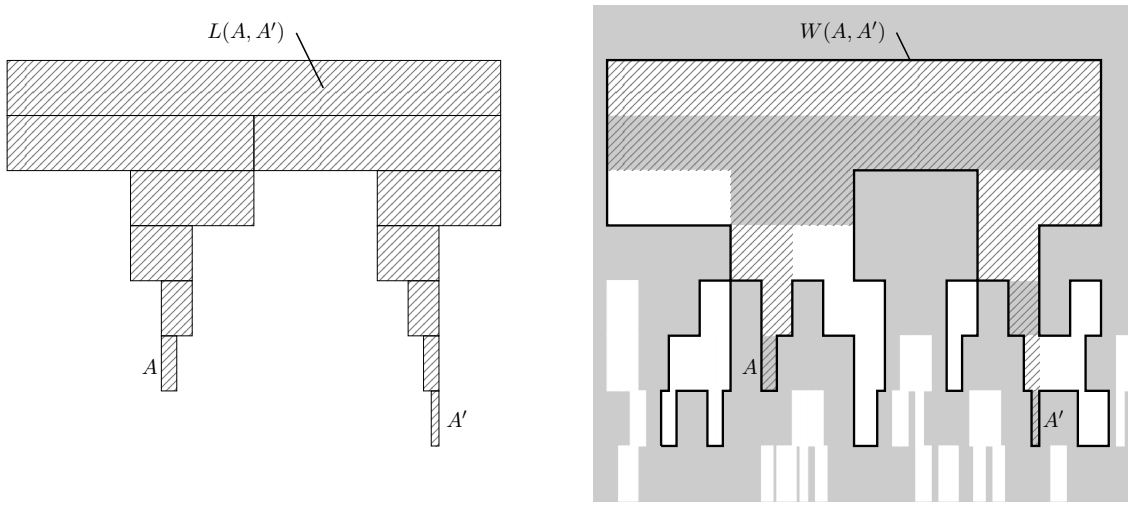

Figure 3.7: Two boxes A, A' in $\mathcal{B}$ and the path $L(A, A')$ that connects them (left). We can form $L(A, A')$ by concatenating the shortest paths from A and A' to the lowest box lying above both A and A'. In the right image active boxes are colored gray and inactive boxes are colored white. The union of $L(A, A')$ and the inactive components intersecting $L(A, A')$ is called $W(A, A')$ and outlined in black.

From every box in $\mathcal{B}$ there is a path of length $\ell \leq R$ to the unique box in the highest layer L_ℓ. Therefore, for every two boxes $A, A' \in \mathcal{B}$ there exists a path $L(A, A')$ from A to A' of length at most $2R$, consisting of the boxes lying above A or A' (Figure 3.7, left). We define $W(A, A')$ as the set of boxes that either lie in $L(A, A')$ or from which an inactive path exists to a box in $L(A, A')$ (Figure 3.7, right). Note that $W(A, A')$ is a connected subset of $\mathcal{B}$, consisting of all boxes in $L(A, A')$ and all inactive components intersecting $W(A, A')$ (by an inactive component we mean a component of the induced subgraph of $\mathcal{B}$ on the inactive boxes). We will show that if vertices $x \in A$, $x' \in A'$ of Γ lie in the same component of Γ, then their graph-theoretic distance can be bounded in terms of the size of $W(A, A')$. This gives an upper bound on the diameter of each component of Γ.

Lemma 3.2.7. *Let $A, A' \in \mathcal{B}$. If vertices $x \in A$, $x' \in A'$ lie in the same component of Γ, then $d_\Gamma(x, x') \leq 37|W(A, A')|$.*

Proof. We claim that there is a walk $S = S_0, S_1, \ldots, S_n$ in $\mathcal{B}$ from A to A' satisfying

(i) if S_i and S_j are active but S_{i+1}, $\ldots$, S_{j-1} are not, then Γ has vertices $a \in S_i$, $b \in S_j$ that are connected in Γ by a path of length at most 3;

(ii) if S_i is active, then either S_i itself or an inactive box adjacent to S_i belongs to $W(A, A')$.

We define $\mathcal{B}_x$ to be the set of active boxes that contain vertices of the component of Γ that contains x and x'. By assumption we have $A, A' \in \mathcal{B}_x$. If A and A' are the only boxes in $L(A, A')$, then we can take $S = (A, A')$. Now suppose A and A' are the only boxes in $L(A, A')$ that belong to $\mathcal{B}_x$. Then the boxes in between A and A' are either inactive, or they are active but contain vertices of a different component of Γ. The box B in $L(A, A')$ directly following A must be inactive and belongs to some inactive component F (recall that an inactive component is a component of the induced subgraph of $\mathcal{B}$ on the inactive boxes). We will prove the stronger statement that a walk $S = S_0, S_1, \ldots, S_n$ from A to A' exists satisfying (i) and

(ii') if S_i is active, then S_i is adjacent to a box in F.

By Lemma 3.2.6 there exists a walk S from A to A' satisfying (i). We will modify S such that also (ii') holds. We proceed in two steps. In Step 1 we modify S such that all inactive boxes in S that are not in F are removed. In Step 2 we remove all active boxes from S that are not adjacent to a box in F.

Step 1. There is a walk S satisfying (i) that contains no inactive boxes outside F.

We start with the walk S that Lemma 3.2.6 provides. This walk satisfies (i). Suppose S contains some inactive box X not in F (Figure 3.8, left). Because $B \in F$, there can then be no inactive path in $\mathcal{B}$ from X to B. It follows from Lemma 3.2.4 that there is an active walk Q that intersects all walks in $\mathcal{B}$ from X to B (we apply Lemma 3.2.4 with the inactive boxes colored blue and all other boxes colored red). One such walk is obtained by following S towards A (which is a neighbor of B). Another possible walk is obtained by first following S towards A' and then following $L(A, A')$ towards B. We define boxes E and E' such that Q intersects the walk in $\mathcal{B}$ from X to B via S and A in E and the walk in $\mathcal{B}$ from X to B via S, A' and $L(A, A')$ in E' (Figure 3.8, left). Because E belongs to S, E also belongs to $\mathcal{B}_x$. It follows that E' also belongs to $\mathcal{B}_x$, which implies that E' lies in S (the boxes in $L(A, A')$ between A and A' do not lie in $\mathcal{B}_x$ by assumption). We see that Q contains two active boxes E and E' that lie on either side of X. Because Q contains only active boxes, we can replace the part of S from E to E' by a walk of active boxes from E to E'. Doing so we find a walk that still satisfies (i) but from which the box X is removed. By repeatedly applying this procedure, we remove all such boxes X from S. The resulting walk satisfies (i) and contains no inactive boxes outside F.

Step 2. There is a walk S satisfying (i) that contains no active boxes outside F', where F' is the set of active boxes adjacent to a box in F.

We start with the walk constructed in Step 1. Since A is adjacent to B it belongs to F'. Let B' be the box in $L(A, A')$ directly preceding A'. We claim that B' belongs to F. Note that B' is inactive. We use Lemma 3.2.4 to show that an inactive path from B to B' exists. If such a path would not exist, then an active walk Q would exist that intersects all walks from B to B'. In particular, Q would contain an active box in $L(A, A') \setminus \{A, A'\}$ (which does not lie in $\mathcal{B}_x$, because by assumption A and A' are the only boxes in $L(A, A')$ that belong to $\mathcal{B}_x$) and an active box in S (which lies in $\mathcal{B}_x$, because we know there is a path in Γ from a vertex in this box to a vertex in A). This is a contradiction, because by Lemma 3.2.3(i) there cannot be an active walk between an active box in $\mathcal{B}_x$ and an active box not in $\mathcal{B}_x$. It follows that an inactive path from B to B' exists, so B' belongs to F. Furthermore, every box in S that has an inactive neighbor in S also lies in F', because this inactive neighbor lies in F by Step 1.

Now consider active boxes S_i, S_{i+1}, ..., S_j in S such that S_i and S_j lie in F' but S_{i+1}, ..., S_{j-1} do not (Figure 3.8, right). We claim that there is a path in F' from S_i to S_j. Color all boxes in F' blue and all other boxes red. Then our claim is that $\mathcal{B}$ contains a blue path from S_i to S_j. We use Lemma 3.2.4 and argue by contradiction. If this blue path would not exist, then there

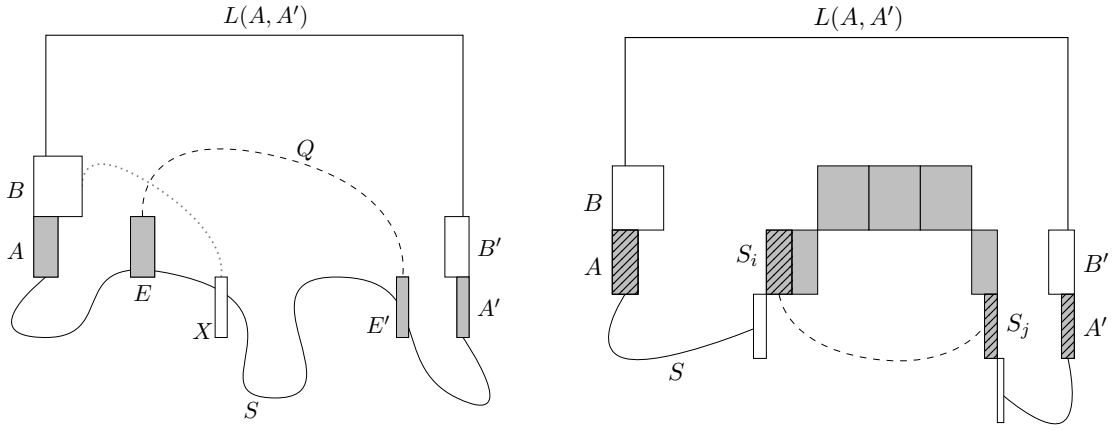

Figure 3.8: Proof of Lemma 8. Left: Step 1. The walk S satisfies (i) and connects A with A'. If from an inactive box X there is no inactive path to B (dotted line), then there is an active walk Q (dashed line) that connects active boxes E and E' in S on either side of X. Right: Step 2. The walk S satisfies (i) and contains no inactive boxes outside F. The boxes A, S_i, S_j and A' (striped) all belong to F'. The proof works by finding a path in F' from S_i to S_j (dashed line). In both figures active boxes are colored gray and inactive boxes are colored white.

would exist a red walk Q that intersects every walk from S_i to S_j. Because S_i and S_j lie in F', there exists such a walk that apart from S_i and S_j contains only boxes in F. Because Q does not contain S_i and S_j (which are blue) it must contain a box in F. Furthermore, Q also contains one of the active boxes $S_{i+1}, \ldots, S_j$. Therefore, Q is a connected set of boxes that contains a box in F and an active box. This implies that Q must also contain a box in F', which contradicts the fact that Q consists of red boxes. This contradiction shows that there must be a blue path in $\mathcal{B}$ from S_i to S_j, i.e. a path in F' from S_i to S_j. We replace the boxes $S_{i+1}, \ldots, S_{j-1}$ of S by this path, thereby removing the boxes $S_{i+1}, \ldots, S_{j-1}$ from S. Repeatedly applying this operation, we remove all active boxes that do not lie in F' from S. This completes Step 2.

The walk constructed in Step 2 satisfies (i) and (ii'), so we are now done with the case that $L(A, A')$ contains no boxes in $\mathcal{B}_x$ other than A and A'.

Now suppose A and A' are not the only boxes in $L(A, A')$ that belong to $\mathcal{B}_x$; let $A = A_0, A_1, \ldots, A_n = A'$ be all the boxes in $L(A, A')$ that belong to $\mathcal{B}_x$ (ordered by their position in $L(A, A')$). All these boxes contain vertices in the same component of Γ. For all i we have $L(A_i, A_{i+1}) \subset L(A, A')$ and furthermore A_i and A_{i+1} are the only boxes in $L(A_i, A_{i+1})$ that belong to $\mathcal{B}_x$. Therefore, a walk from A_i to A_{i+1} satisfying (i) and (ii) exists. By concatenating these walks for all i we find a walk S from A to A' satisfying (i) and (ii).

We now construct a path in Γ from x to x' of length at most $37|W(A, A')|$. We may assume that the active boxes in S are all distinct, because if S contains an active box twice we can remove the intermediate part of S. The number of active boxes in S is at most $9|W(A, A')|$ because each active box in S lies in $W(A, A')$ or is one of the at most 8 neighbors of an inactive box in $W(A, A')$. Suppose S_i and S_j are active boxes in S such that $S_{i+1}, \ldots, S_{j-1}$ are all inactive. Then for every vertex $v \in S_i$ there is a path in Γ of length at most 4 to a vertex in S_j: by (i) there are vertices $a \in S_i$, $b \in S_j$ such that $d_\Gamma(a, b) \leq 3$ and furthermore v and a are neighbors because they lie in the same box. It follows that there is a path of length at most $36|W(A, A')|$ from x to a vertex in A', hence a path of length at most $36|W(A, A')| + 1 \leq 37|W(A, A')|$ from x to x'. □

Bounding the diameter

In this paragraph, we use the results from the previous paragraph to prove that for $\alpha = 1$ and ν sufficiently large, as well as for $\alpha \in (\frac{1}{2}, 1)$ and ν arbitrary, a.a.s. all components of the graphs $G(N; \alpha, \nu)$ and $G_{\mathrm{Po}}(N; \alpha, \nu)$ have diameter $O(R) = O(\log(N))$. We first show that when $\lambda = \frac{\nu\alpha}{\pi}$, Γ_λ^Δ (the subgraph of Γ_λ induced by the vertices with y-coordinate at most $R/2$) satisfies the conditions in the Lemma below. In particular, this would imply that a.a.s. all components of Γ_λ^Δ have diameter $O(R)$. In the final part of this paragraph we translate this result to the KPKVB model.

Lemma 3.2.8. *Let $V \subset \mathcal{E}_R$ be a finite set of points and let Γ be the graph with vertex set V and connection rule $(x, y) \sim (x', y') \iff |x - x'|_{\pi e^{R/2}} \leq e^{\frac{1}{2}(y+y')}$. Let $K = \{(x, y) \in \mathcal{E}_R : y > R/4\}$. Consider the following two conditions:*

(i) For any two boxes A and A' we have $|W(A, A')| = O(R)$;

(ii) There is no inactive path in $\mathcal{B}$ connecting a box in L_0 with a box in K.

If (i) holds, then each component of Γ has diameter $O(R)$. If furthermore (ii) holds, then the same holds for any graph Γ' that is obtained from Γ by adding a number of edges, each of which has an endpoint in K.

Proof. The first statement is a direct consequence of Lemma 3.2.7.

If furthermore (ii) holds, there exists a cycle of active boxes in $\mathcal{E}_R \backslash K$ that separates K from L_0. Since vertices in neighboring boxes are connected in Γ, this means that there is a cycle in Γ that separates K from L_0. Every vertex in K lies above some edge in this cycle and thereby lies in the component C of this cycle by Lemma 3.2.5(i). Thus, every edge of Γ' that is not present in Γ has an endpoint in the component C of Γ.

Let d be the maximum diameter over all components of Γ. We claim that every component of Γ' has diameter at most $3d + 2$. This is clear for a component of Γ' disjoint with C, because such a component is also a component of Γ. In the component of Γ' containing C there exists a path of length at most $d + 1$ from each vertex to a vertex in C. Since C has diameter at most d, it follows that this component indeed has diameter at most $3d + 2$. This implies that if every component of Γ has diameter $O(R)$, then every component of Γ' also has diameter $O(R)$. □

We start by showing that Γ_λ^Δ has property (i) of Lemma 3.2.8. To do so, we need to estimate the probability that a box is inactive if the graph Γ is given by Γ_λ (i.e. if V is the point set V_λ of the Poisson process $\mathcal{P}_{\alpha,\lambda}$).

Lemma 3.2.9. *If $\Gamma = \Gamma_\lambda$, then the probability that a box in layer L_i is inactive (i.e. contains no vertex of Γ) is at most $\exp(-\frac{1}{12} \cdot \lambda \cdot 2^{(1-\alpha)i})$. The same bound holds if $\Gamma = \Gamma_\lambda^\Delta$ and L_i lies below the line $y = R/2$.*

Proof. The expected number of points of $\mathcal{P}_{\alpha,\lambda}$ that fall inside a box B in layer L_i satisfies

$$\mathbb{E}(|B \cap \mathcal{P}_{\alpha,\lambda}|) \geq \int_{i\log(2)}^{(i+1)\log(2)} \int_0^{2^i b} \lambda e^{-\alpha y} \,\mathrm{d}x \,\mathrm{d}y = \lambda \cdot b \cdot \frac{1 - 2^{-\alpha}}{\alpha} \cdot 2^{(1-\alpha)i}$$

(this is an equality for $i < \ell$). Therefore, the probability that B contains no vertices of Γ_λ is bounded by $\exp(-\lambda \cdot b \cdot \frac{1-2^{-\alpha}}{\alpha} \cdot 2^{(1-\alpha)i}) \leq \exp(-\frac{1}{12} \cdot \lambda \cdot 2^{(1-\alpha)i})$ because $b \cdot \frac{1-2^{-\alpha}}{\alpha} \geq \frac{1}{12}$. The second part follows immediately from the first part, because Γ_λ^Δ is the subgraph of Γ_λ induced by the vertices below the line $y = R/2$. □

If $\alpha = 1$, Lemma 3.2.9 tells us that for $\Gamma = \Gamma_\lambda^\Delta$, every box below the line $y = R/2$ is inactive with probability at most $\exp(-\frac{\lambda}{12})$. The at most 63 boxes (partly) above the line $y = R/2$ are inactive with higher probability, because in Γ_λ^Δ the vertices with y-coordinate exceeding $R/2$ are removed. If a box lies completely above the line $y = R/2$ it is even always inactive.

Lemma 3.2.10. *Let $\alpha = 1$ and let λ be sufficiently large. Then if $\Gamma = \Gamma_\lambda^\Delta$ it holds with probability $1 - O(N^{-1})$ that for any two boxes A and A' we have $|W(A, A')| = O(R)$.*

Proof. We show that the probability that there are boxes A and A' which satisfy $|W(A, A')| > 32R$ is $O(N^{-1})$. Suppose that $|W(A, A')| > 32R$ for two boxes A and A'. Since $W(A, A')$ is a connected subgraph of $\mathcal{B}$, there exists a walk P, starting at A, through all boxes in $W(A, A')$, that uses no edge in $\mathcal{B}$ more than twice (this is a general property of a connected graph). Because no box has more than 8 neighbors, P visits no box more than 8 times. Therefore, the first $32R$ steps of P (which exist since $|W(A, A')| > 32R$) pass through at least $32R/8 = 4R$ distinct boxes, of which at least $4R - 2R - 63 \geq R$ are inactive and lie below the line $y = R/2$ (we subtract the at most $2R$ boxes in $L(A, A')$ and the at most 63 boxes partly above the line $y = R/2$; the estimate $R \geq 63$ of course holds for sufficiently large R). The probability that these boxes are indeed inactive is bounded by $\exp(-\lambda/12 \cdot R) = \exp(-\lambda R/12)$, because by Lemma 3.2.9, $\exp(-\lambda/12)$ is an upper bound for the probability that a box below the line $y = R/2$ is inactive.

The walk P can be chosen in at most 9^{32R} ways. Therefore, the probability that $|W(A, A')| > 32R$ for some boxes A and A' (which can be chosen in at most $O(e^R)$ ways) is at most

$$O(e^R)9^{32R}\exp(-\lambda R/12) = \exp(O(R) - \lambda R/12) \leq \exp(-R/2) = O(N^{-1}),$$

where the inequality holds for sufficiently large λ. □

We now want to show that for the graph Γ_λ^Δ the estimate $|W(A, A')| = O(R)$ also holds a.a.s. when $\alpha \in (\frac{1}{2}, 1)$ and λ is arbitrary. The probability that a box in layer i is inactive is bounded by $\exp(-\frac{\lambda}{12}2^{(1-\alpha)i})$ (this bound now depends on i), which decreases rapidly if i increases. However, for low values of i and λ this expression can be arbitrarily close to 1. To gain control over the boxes in the lowest layers, we merge boxes in the lowest layers into larger blocks.

An *h-block* is defined as the union of a box in L_{h-1} and all $2^h - 2$ boxes lying below this box (Figure 3.9, left). In other words, an h-block consists of $2^h - 1$ boxes in the lowest h layers that together form a rectangle. The following Lemma shows that the probability that an h-block contains a horizontal inactive path can be made arbitrarily small by taking h large.

Lemma 3.2.11. *Let $\alpha < 1$ and let p_h be the probability that an h-block contains a horizontal inactive path (that is, a path in $\mathcal{B}$ of inactive boxes connecting a box touching its left edge to a box touching its right edge). For the graph Γ_λ^Δ we have $p_h \to 0$ as $h \to \infty$.*
(Here we always assume that $(h + 1)\log 2 \leq R/2$, to make sure that the h-blocks we consider do not extend above the line $y = R/2$.)

Proof. Because the boxes we consider do not extend above the line $y = R/2$, we can use Lemma 3.2.9 to estimate the probability that a box is inactive.

An $(h+1)$-block H consists of one box B in layer L_h and two h-blocks B_1, B_2. If H is inactive, then B is inactive or both B_1 and B_2 are inactive. It follows that

$$p_{h+1} \leq \exp(-\tfrac{\lambda}{12}\gamma^h) + p_h^2 \leq \max(2\exp(-\tfrac{\lambda}{12}\gamma^h), 2p_h^2),$$

because B is inactive with probability at most $\exp(-\frac{\lambda}{12}\gamma^h)$, where $\gamma = 2^{1-\alpha} \in (1, 2)$. Writing $p_h = e^{-y_h}/2$, we see that $y_{h+1} \geq \min\left(\frac{\lambda}{12}\gamma^h - \log(4), 2y_h\right)$. We will show that this implies $y_h \to \infty$. There exists an h_0 such that $\frac{\lambda}{12}\gamma^{h-1}(2 - \gamma) \geq \log(4)$ for $h \geq h_0$. If for some $n \geq h_0$ we have

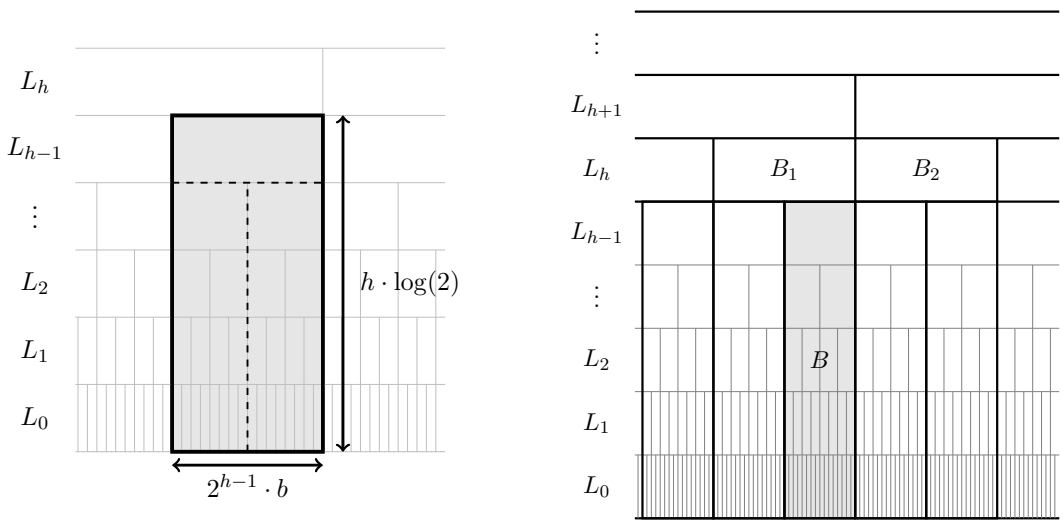

Figure 3.9: Left: an h-block (in the figure $h = 5$). An h-block is the union of $2^h - 1$ boxes in the lowest h layers. Right: definition of a lonely block (used in the proof of Lemma 3.2.12). The lowest h layers are partitioned into h-blocks. An h-block B in W' is called *lonely* if both boxes B_1 and B_2 lying above it are not in W'. If $|W'| > 3$ and B is lonely, one of the blocks adjacent to B contains a horizontal path in W.

$y_n \geq \frac{\lambda}{12}\gamma^{n-1} - \log(4)$, then it follows that $y_{n+1} \geq \frac{\lambda}{12}\gamma^n - \log(4)$ or $y_{n+1} \geq 2y_n \geq 2(\frac{\lambda}{12}\gamma^{n-1} - \log(4)) \geq \frac{\lambda}{12}\gamma^n - \log(4)$. By induction, we then find $y_h \geq \frac{\lambda}{12}\gamma^{h-1} - \log(4)$ for all $h \geq n$, showing that $y_h \to \infty$. If not, we have $y_n \geq 2y_{n-1}$ for all $n \geq h_0$ and it follows that $y_h \geq 2^h 2^{-h_0} y_{h_0}$ for all $h \geq h_0$. In that case we also clearly have $y_h \to \infty$. □

Lemma 3.2.12. *Let $\alpha \in (\frac{1}{2}, 1)$ and let λ be arbitrary. Then for Γ_λ^Δ it holds with probability $1 - O(N^{-1})$ that for any two boxes A and A' we have $|W(A, A')| = O(R)$.*

Proof. Let p_h be the probability that an h-block contains a horizontal inactive path and let q_h be the maximum probability that a box outside the lowest h layers (but below the line $y = R/2$) is inactive. Since $q_h \leq \exp(-\frac{\lambda}{12} \cdot 2^{(1-\alpha)h})$ by Lemma 3.2.9, we have $q_h \to 0$ as $h \to \infty$. By Lemma 3.2.11 we also have $p_h \to 0$ for $h \to \infty$. Therefore, we can choose h such that $\max(p_h, q_h) < 9^{-1104} e^{-3/2}$. As in Lemma 3.2.11, for sufficiently large R, all h-blocks lie completely below the line $y = R/2$.

We need to show that that

$$\mathbb{P}\left(|W(A, A')| \leq CR \text{ for all } A, A' \in \mathcal{B}\right) = 1 - O(N^{-1})$$

for some constant C. We take $C = 1104(2^h - 1)$ for the value of h specified above.

We replace the boxes in the h lowest layers by h-blocks. These h-blocks and the boxes above the lowest h layers together are the vertex set of a graph $\mathcal{B}'$, where boxes or blocks are neighbors if they share at least a corner. Note that the maximum degree of $\mathcal{B}'$ is at most 8. Furthermore, if $W \geq CR$ then $W' \geq 1104R$, where W' is the corresponding connected subset of $\mathcal{B}'$. In $\mathcal{B}'$ there exists a walk P through all boxes and blocks in W' that visits no box or block more than 8 times. The first $1104R$ steps of the walk P can be chosen in at most 9^{1104R} ways.

For a given choice of P (and hence W') we let r denote the number of blocks in P and s denote the number of boxes in P. We have $r + s = 1104R$. We will now estimate the probability that these boxes and blocks indeed occur as W'.

First suppose $s \geq 32R$. Because each box occurs at most 8 times in P, this means that W' contains at least $4R$ distinct boxes. After subtracting the at most $2R$ boxes in $L(A, A')$ and the

at most 63 boxes (partly) above the line $y = R/2$, we find that there are at least R inactive boxes in W' that lie below the line $y = R/2$. The probability that these boxes (which are specified by our choice of P) are indeed inactive, is at most q_h^R.

If $s < 32R$ we must have $r \geq 1072R$. We now count *lonely* blocks, which we define as blocks B for which the two boxes in L_h adjacent to B both do not lie in W (Figure 3.9, right). Since there are at most s boxes in L_h, there are at most $4s$ blocks that are not lonely (each box in L_h is adjacent to 4 blocks). Since there are at least $\frac{r}{8}$ distinct blocks in W, there are at least $\frac{r}{8} - 4s = \frac{r-32s}{8} = \frac{33r-32(r+s)}{8} \geq \frac{33\cdot 1072R - 32\cdot 1104R}{8} = 6R$ lonely blocks. If we assume $|W'| > 3$ then for each lonely block B, one of the two blocks adjacent to B must contain a horizontal path in W. Since each block is adjacent to 2 other blocks, there are at least $3R$ blocks in W' that contain a horizontal path in W. Since there are at most 2 blocks in $L(A, A')$, there are at least $3R - 2 \geq R$ blocks in W' that contain a horizontal inactive path. The probability that this happens is at most p_h^R.

Noting that there are $O(e^R)$ pairs of boxes, we see that

$$\begin{aligned}\mathbb{P}(|W(A, A')| > CR \text{ for some } A, A' \in \mathcal{B}) &\leq O(e^R) \cdot 9^{1104R} \cdot \max(q_h^R, p_h^R) \\ &= O((9^{1104} e \max(p_h, q_h))^R) = O(e^{-R/2}) = O(N^{-1})\end{aligned}$$

because we chose h such that $9^{1104} e \max(p_h, q_h) < e^{-1/2}$. □

We now turn to the proof of (ii) of Lemma 3.2.8.

Lemma 3.2.13. *Suppose that $\alpha = 1$ and λ is sufficiently large. Then if $\Gamma = \Gamma_\lambda^\Delta$ it holds with probability $1 - O(N^{-1})$ that there are no inactive paths in $\mathcal{B}$ from L_0 to K, where $K = \{(x, y) \in \mathcal{E}_R : y > R/4\}$. The same holds for $\alpha \in (\frac{1}{2}, 1)$ and λ arbitrary.*

Proof. Since only the boxes below the line $y = R/2$ are relevant, we can freely use Lemma 3.2.9. Note that an inactive path in $\mathcal{B}$ from L_0 to K would have length at least $R/4$ (the height of each layer equals $\log 2 < 1$) and that it would have a subpath of length at least $R/8$ that lies completely in $\{(x, y) : y > R/8\}$. Let q be the maximum probability that a box between the lines $y = R/8$ and $y = R/2$ is inactive. Since there are $\exp(O(R))$ boxes and at most 9^k paths of length k starting at any given box, the probability that such a subpath exists is at most $\exp(O(R))9^{R/8}q^{R/8} = \exp(O(R) + \log(q)R/8)$. If $\alpha = 1$ then $q \leq \exp(-\lambda/12)$, which can be chosen arbitrarily small by choosing λ sufficiently large. For sufficiently small q we then have $\exp(O(R) + \log(q)R/8) \leq \exp(-R/2) = O(N^{-1})$ and therefore such a path does not exist with probability $1 - O(N^{-1})$. If $\alpha < 1$ we have $q \leq \exp(-\lambda/12 \cdot 2^{(1-\alpha)R/8})$ and it follows that $\exp(O(R) + \log(q)R/8) = \exp(O(R) - \lambda/12 \cdot 2^{(1-\alpha)R/8} \cdot R/8) \leq \exp(-R/2)$ for sufficiently large R, so we can draw the same conclusion. □

We can now prove Theorem 3.2.1 for the Poissonized version of the model.

Theorem 3.2.14 (Theorem 3.2.1 for G_{Po})**.** *Let $\alpha, \nu > 0$. Then the following holds:*

(i) For $\frac{1}{2} < \alpha < 1$ and ν arbitrary, a.a.s. every component of $G_{\text{Po}}(N; \alpha, \nu)$ has diameter $O(\log(N))$.

(ii) For $\alpha = 1$ and ν sufficiently large, a.a.s. every component of $G_{\text{Po}}(N; \alpha, \nu)$ has diameter $O(\log(N))$.

Proof. We first deal with (i), so suppose $\alpha \in (\frac{1}{2}, 1)$ and ν is arbitrary. By Lemma 3.2.2, it suffices to prove that a.a.s. every component of G_{Po}^Δ has diameter $O(\log N)$. By Lemma 2.3.1 and Lemma 2.3.2, a.a.s. a graph isomorphic to G_{Po}^Δ can be obtained from $\Gamma_{\nu\alpha/\pi}^\Delta$ by adding a number of edges, each of which has an endpoint in $K = \{(x, y) \in \mathcal{E}_R : y > R/4\}$. Lemma 3.2.8 will now

show that a.a.s. every component of G^{Δ}_{Po} (and hence also G_{Po}) has diameter $O(\log N)$ (recall that $R = O(\log N)$). Indeed, Lemma 3.2.12 shows that $\Gamma^{\Delta}_{\nu\alpha/\pi}$ satisfies condition (i) of Lemma 3.2.8, and Lemma 3.2.13 shows that $\Gamma^{\Delta}_{\nu\alpha/\pi}$ satisfies condition (ii) of Lemma 3.2.8. The proof is complete.

The argument for (ii), where $\alpha = 1$ and ν (hence $\lambda = \nu\alpha/\pi$) is sufficiently large, is identical. For the conditions of Lemma 3.2.8, we now refer to Lemma 3.2.10 and Lemma 3.2.13. □

Finally, we give a proof of Theorem 3.2.1.

Proof. Assume α and ν satisfy the conditions of this theorem, i.e. $\alpha = 1$ and ν is sufficiently large or $\alpha \in (\frac{1}{2}, 1)$ and ν is arbitrary. By Lemma 3.2.2, it suffices to show that a.a.s. every component of the graph G^{Δ} has diameter $O(\log N)$. In light of Lemma 2.3.3 and 2.3.4, it now suffices to show that when conditioned on $Z = N$, $\Gamma^{\Delta}_{\nu\alpha/\pi}$ a.a.s. satisfies the conditions (i) and (ii) of Lemma 3.2.8. By Lemma 3.2.10, Lemma 3.2.12 and Lemma 3.2.13, $\Gamma^{\Delta}_{\nu\alpha/\pi}$ satisfies conditions (i) and (ii) with probability at least $1 - O(N^{-1})$. The desired result now follows from applying Lemma 2.1.1. □

Discussion

In this thesis we have discussed the KPKVB model, a random geometric graph model in the hyperbolic plane that has characteristics reminiscent of complex networks. The original contribution of the thesis is a proof of a logarithmic upper bound for the diameter in this model, which holds with probability tending to 1 as the number of vertices tends to infinity. This proof was provided in Section 3.2. Together with an already known lower bound [19, 12], which we presented in Section 3.1, this leads to the following precise statement: for fixed values of $\alpha \in (\frac{1}{2}, 1)$ and $\nu > 0$, there are constants C_1 and C_2 such that with probability tending to 1, the maximum diameter of all components in the KPKVB model lies between $C_1 \log N$ and $C_2 \log N$. Put differently, when the power law exponent is between 2 and 3, the diameter in the KPKVB model is logarithmic in the number of vertices. This makes the diameter of the KPKVB model similar to that of other models for complex networks, such as the Chung–Lu model, and emphasizes the "small-world" property of the model.

A natural remaining question is what happens for values of α outside $(\frac{1}{2}, 1)$. These regimes are of less importance for network scientists (power law exponents are usually found between 2 and 3 in practice), but equally interesting from a mathematical perspective. The lower bound provided in Section 3.1 works for all values of $\alpha > \frac{1}{2}$. Our upper bound also works for $\alpha = 1$ and large values of ν, so this case is also settled. The only thing we have proven for $\alpha > 1$ or $\alpha = 1$ and small ν (values for which the giant component disappears) is that there are components of logarithmic diameter. However, it may be the case that for these parameter values there are components of even larger diameter. For $\alpha < \frac{1}{2}$ the diameter is known to be constant (see Section 2.1); the case $\alpha = \frac{1}{2}$ also remains open.

For $\alpha \in (\frac{1}{2}, 1)$ the asymptotic upper and lower bound for the diameter differ by a multiplicative constant. It would be interesting to further close this gap. It might be the case that there exists some function $C(\alpha, \nu)$ such that the diameter tends to $C(\alpha, \nu) \log N$ in probability (this would be a result similar in flavor to recent results on the size of the largest component [11]). One could also wonder how the diameter depends on the values of α and ν. For this purpose, a careful analysis of the proofs in Chapter 3 would be instructive.

The strategy used in the proof of the upper bound for the diameter may be applicable to a broader range of random geometric graphs. The main ingredients we used in the proof are the properties of our discretized model, summarized in Lemma 3.2.3, and the geometric properties of Lemma 3.2.5. If a random geometric graph is given in which points are connected if they have at most a certain distance from each at other (which is not the case for our idealized model), then Lemma 3.2.5 follows immediately from the triangle inequality. The conditions on the dissection (Lemma 3.2.3) also seem flexible enough to be true for other random geometric graph models.

Index

Bibliography

[1] M. A. Abdullah, M. Bode, and N. Fountoulakis. Typical distances in a geometric model for complex networks, 2015. Preprint. ArXiV version: `https://arxiv.org/abs/1506.07811`.

[2] A.-L. Barabási and R. Albert. Emergence of scaling in random networks. *Science*, 286(5439):509–512, 1999.

[3] M. Bode, N. Fountoulakis, and T. Müller. On the largest component of a hyperbolic model of complex networks. *The Electronic Journal of Combinatorics*, 22(3):P3.24, 2015.

[4] M. Bode, N. Fountoulakis, and T. Müller. The probability of connectivity in a hyperbolic model of complex networks. *Random Structures & Algorithms*, 49(1):65–94, 2016.

[5] M. Boguñá, F. Papadopoulos, and D. Krioukov. Sustaining the internet with hyperbolic mapping. *Nature Communications*, 1:62, 2010.

[6] B. Bollobás and O. Riordan. *Percolation*. Cambridge University Press, 2006.

[7] F. Chung and L. Lu. The average distances in random graphs with given expected degrees. *Proceedings of the National Academy of Sciences*, 99(25):15879–15882, 2002.

[8] H. S. M. Coxeter and S. L. Greitzer. *Geometry Revisited*. Mathematical Association of America, 1967.

[9] S. Dommers, R. van der Hofstad, and G. Hooghiemstra. Diameters in preferential attachment models. *Journal of Statistical Physics*, 139(1):72–107, 2010.

[10] P. Flajolet and R. Sedgewick. *Analytic Combinatorics*. Cambridge University Press, 2009.

[11] N. Fountoulakis and T. Müller. Law of large numbers for the largest component in a hyperbolic model of complex networks, 2016. Preprint. ArXiv version: `https://arxiv.org/pdf/1604.02118v2.pdf`.

[12] T. Friedrich and A. Krohmer. On the diameter of hyperbolic random graphs. In M. M. Halldórsson, K. Iwama, N. Kobayashi, and B. Speckmann, editors, *Automata, Languages, and Programming: 42nd International Colloquium, ICALP 2015, Kyoto, Japan, July 6-10, 2015, Proceedings, Part II*, pages 614–625, Springer Berlin Heidelberg, 2015. ArXiv version: `https://arxiv.org/abs/1512.00184`.

[13] G. García-Pérez, M. Boguñá, A. Allard, and M. Á. Serrano. The hidden hyperbolic geometry of international trade: World trade atlas 1870–2013. *Scientific Reports*, 6:33441, 2016.

[14] L. Gugelmann, K. Panagiotou, and U. Peter. Random hyperbolic graphs: Degree sequence and clustering. In A. Czumaj, K. Mehlhorn, A. Pitts, and R. Wattenhofer, editors, *Automata, Languages, and Programming: 39th International Colloquium, ICALP 2012, Warwick, UK, July 9-13, 2012, Proceedings, Part II*, pages 573–585, Springer Berlin Heidelberg, 2012. ArXiv version: `https://arxiv.org/abs/1205.1470`.

[15] R. Guimerá and L. A. N. Amaral. Modeling the world-wide airport network. *The European Physical Journal B*, 38(2):381–385, 2004.

[16] D. Hilbert. Über Flächen von konstanter Krümmung. *Transactions of the American Mathematical Society*, 2:87–99, 1901.

[17] H. Kesten. *Percolation theory for mathematicians*. Birkhäuser, Boston, 1982.

[18] J. F. C. Kingman. *Poisson Processes*. Oxford Studies in Probability. Clarendon Press, 1993.

[19] M. Kiwi and D. Mitsche. A bound for the diameter of random hyperbolic graphs. In *Proceedings of the Meeting on Analytic Algorithmics and Combinatorics*, pages 26–39, SIAM, 2015. ArXiv version: `https://arxiv.org/abs/1408.2947`.

[20] D. Krioukov, M. Kitsak, R. S. Sinkovits, D. Rideout, D. Meyer, and M. Boguñá. Network cosmology. *Scientific Reports*, 2:793, 2012.

[21] D. Krioukov, F. Papadopoulos, M. Kitsak, A. Vahdat, and M. Boguñá. Hyperbolic geometry of complex networks. *Physical Review E*, 82:036106, 2010.

[22] S. Lang. *Complex Analysis*. Graduate Texts in Mathematics. Springer New York, 2003.

[23] S. Milgram. The small world problem. *Psychology Today*, pages 60–67, 1967.

[24] J. Stillwell. *Geometry of Surfaces*. Universitext. Springer New York, 1992.

[25] S. H. Strogatz. Exploring complex networks. *Nature*, 410:268–276, 2001.

[26] R. Van der Hofstad. Random graphs and complex networks (lecture notes), 2014. Last accessed February 12, 2017. Online version: `http://www.win.tue.nl/~rhofstad/NotesRGCN.pdf`.

[27] C. Walkden. Hyperbolic geometry (lecture notes), 2017. Last accessed February 3, 2017. Online version: `http://www.maths.manchester.ac.uk/~cwalkden/hyperbolic-geometry/hyperbolic_geometry.pdf`.

[28] D. J. Watts and S. H. Strogatz. Collective dynamics of "small-world" networks. *Nature*, 393:440–442, 1998.